BAYLOR GEOLOGICAL STUDIES

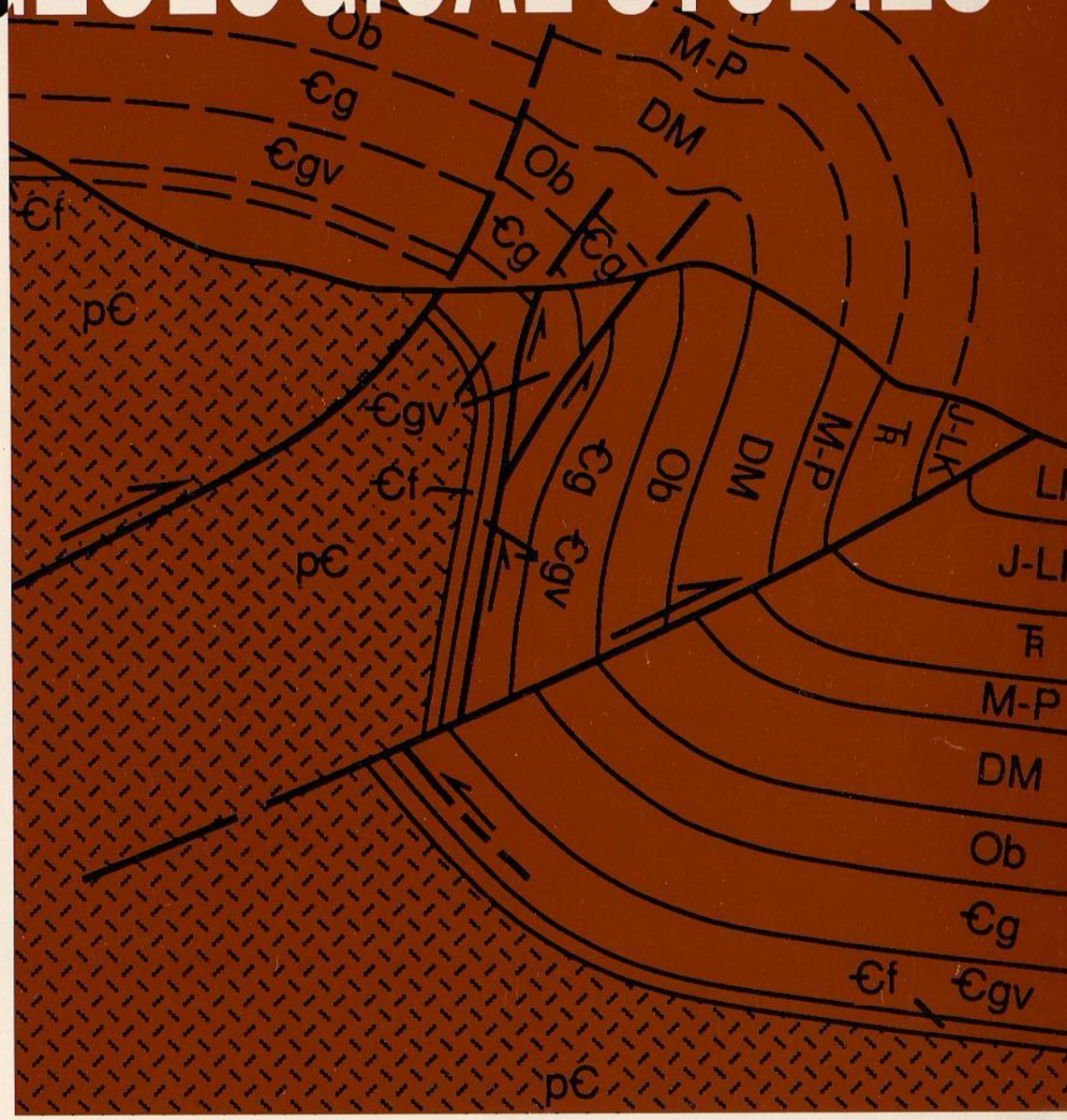

FALL 1995

Bulletin No. 56

Thesis Abstracts

"Creative thinking is more important than elaborate equipment--"

FRANK CARNEY, PH.D.
PROFESSOR OF GEOLOGY
BAYLOR UNIVERSITY
1929-1934

Objectives of Geological Training at Baylor

The training of geologists in a university covers but a few years; their educations continue throughout their active lives. The purposes of training geologists at Baylor University are to provide a sound basis of understanding and to foster a truly geological point of view, both of which are essential for continued professional growth. The staff considers geology to be unique among sciences since it is primarily a field science. All geologic research including that done in laboratories must be firmly supported by field observations. The student is encouraged to develop an inquiring objective attitude and to examine critically all geological concepts and principles. The development of a mature and professional attitude toward geology and geological research is a principal concern of the department.

Cover: The Five Springs structure located along the western front of the Bighorn Mountains of north-central Wyoming (from Willis).

BAYLOR GEOLOGICAL STUDIES

BULLETIN NO. 56

THESIS ABSTRACTS

These abstracts are taken from theses written in partial fulfillment of degree requirements at Baylor University. The original, unpublished versions of the theses, complete with appendices and bibliographies, can be found in the Jesse Jones Library, Baylor University, Waco, Texas.

BAYLOR UNIVERSITY
Department of Geology
Waco, Texas
Fall 1995

Baylor Geological Studies

The Baylor Geological Studies Bulletin is published by the Department of Geology at Baylor University. The Bulletin is specifically dedicated to the dissemination of geologic knowledge for the benefit of the people of Texas. The publication is designed to present the results of both pure and applied research which will ultimately be important in the economic and cultural growth of the State.

ISSN 0005-7266

Additional copies of this bulletin can be obtained from the Department of Geology, PO Box 97354, Baylor University, Waco, Texas 76798.

CONTENTS

Crustal Velocity Structure of Central Texas

Jessie Lafayette Bonner

Structural and velocity models were generated for the crust of Central Texas through the inversion of compressional, shear, and surface wave data recorded at the W.M. Keck Foundation Seismological Observatory (international code BUTX) at Baylor University, Waco, Texas. By determining crustal velocity structure for the region, location of local earthquakes is accomplished more accurately, and a better understanding of the upper crust is obtained. The observatory became operational in April, 1992, and data used in this research were obtained during the first 18 months of operation. The recording of earthquakes from all over the world has allowed the detection limits of the observatory to be established. These limits include: magnitude 1.5 for events in Texas; 3.9 in California; and 4.1 in South Carolina. Earthquakes of magnitude 6.5 or greater at any point in the earth can be detected at the observatory.

Limestone quarries located in several directions from BUTX detonate two to fifteen tons of explosives several times per week. Portable digital acquisition systems were placed at each quarry to determine blast origin times. Recordings of the blasts at BUTX show sharp onset of compressional and shear waves. The compressional phase observed from blasts of epicentral distance less than 30 km is Pg, compressional wave energy which has traveled through the crust directly from source to seismometer. Pg phases produced from quarries in Crawford and Clifton, Texas, have slow velocities, 2.42 and 2.57 km/sec, respectively, indicating a shallow propagation path as well as the absence of dense rock. Pg velocities obtained from regional earthquakes are much faster, with average velocities of 5.47 to 6.07 km/sec, indicating much deeper penetration of the waves into the crust.

Regional earthquakes from western and southern Texas, northern and central Mexico, southern Oklahoma, and offshore Louisiana were studied for their shear wave phase content. The presence or absence of Lg, a continental-guided shear phase, helped determine the deep crustal structure for Central Texas. Earthquakes originating in western Texas, northern Mexico, southern Oklahoma, and southern Texas have maximum energy in the Lg phase, which indicates that the propagation path is dominated by continental crust. Earthquakes recorded from central Mexico have equal amounts of energy in the Lg and Sn (shear energy refracted from the mantle) phases, which suggests a transition between oceanic crust to continental crust approximately half-way along the path. Finally, earthquakes occurring offshore of Louisiana produce only Sn at BUTX, due to a lack of continental crust beneath the Gulf of Mexico.

Shear velocity models of the upper 1.5 km of the Central Texas crust were obtained by inverting dispersed Rayleigh and Love waves from local quarry blasts. Multiple filter analysis techniques (Fig. 1) were used to obtain high-quality dispersion curves for the surface waves, and inversion techniques were applied to produce shear velocity models. Recordings of the blasts from quarries in Crawford and Clifton, Texas, show dispersed Rayleigh waves in the period band 0.22 to 2.0 seconds. Models from dispersion along the Clifton and Crawford path (Fig. 2) show excellent resolution in the upper 0.5 kilometers of the crust. The Washita Group (Cretaceous) was distinguished as the top layer of the velocity model with shear velocities of approximately 1.00 km/sec. A faster section in the model (1.12 km/sec) is caused by the hard limestones of the Edwards and Glen Rose Formations (Cretaceous) of the Fredericksburg and upper Trinity Groups, respectively. A low-velocity layer with shear velocities of only 1.05 km/sec is related to the basal Cretaceous sands of the lower Trinity Group. Inversion of dispersed Love waves from Clifton, Texas, shows a different model from that produced from Rayleigh waves along the same path. Anisotropy in the upper crust causes this phenomenon of different SH and SV velocity structure. Shear wave velocity determined by the inversion of Love waves from blasts in Midlothian, Texas, is faster than along Clifton and Crawford paths, due to the presence of buried, metamorphosed rocks of the Paleozoic Ouachita facies.

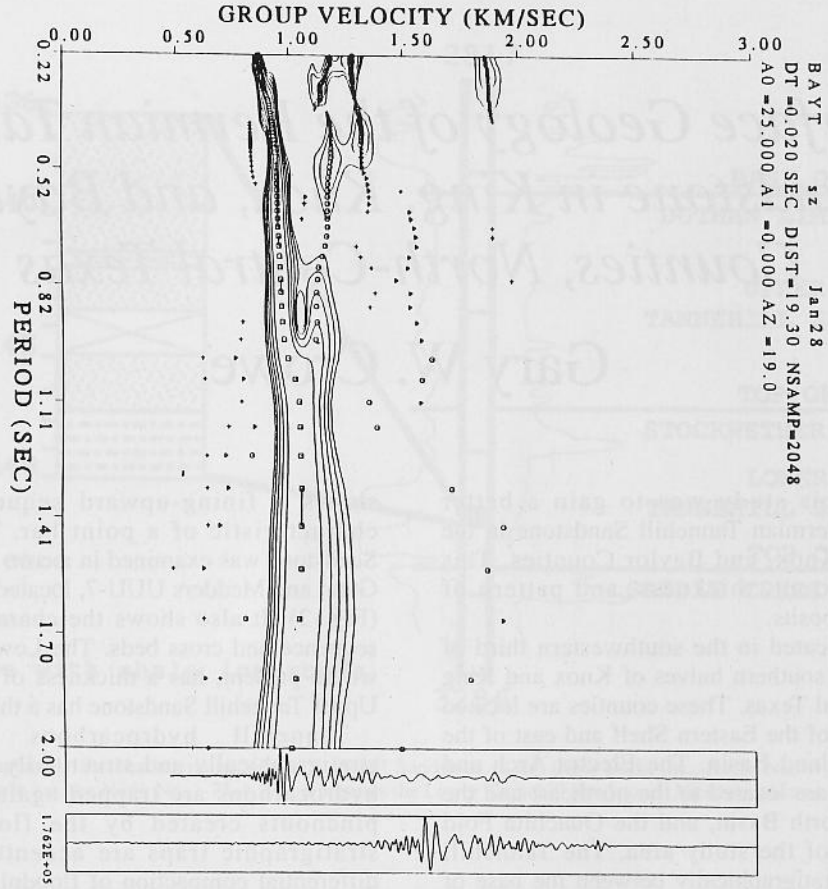

Fig. 1. Multiple Filter Analysis of the short-period vertical component from a Crawford, Texas, quarry blast. Group velocity is determined by dividing the epicentral distance by the travel time for each period of the waveform. Gaussian filters are implemented and the four highest amplitudes at each period are determined and plotted as squares, triangles, circles, or plus signs. The amplitudes are then contoured, and the group velocities are extracted.

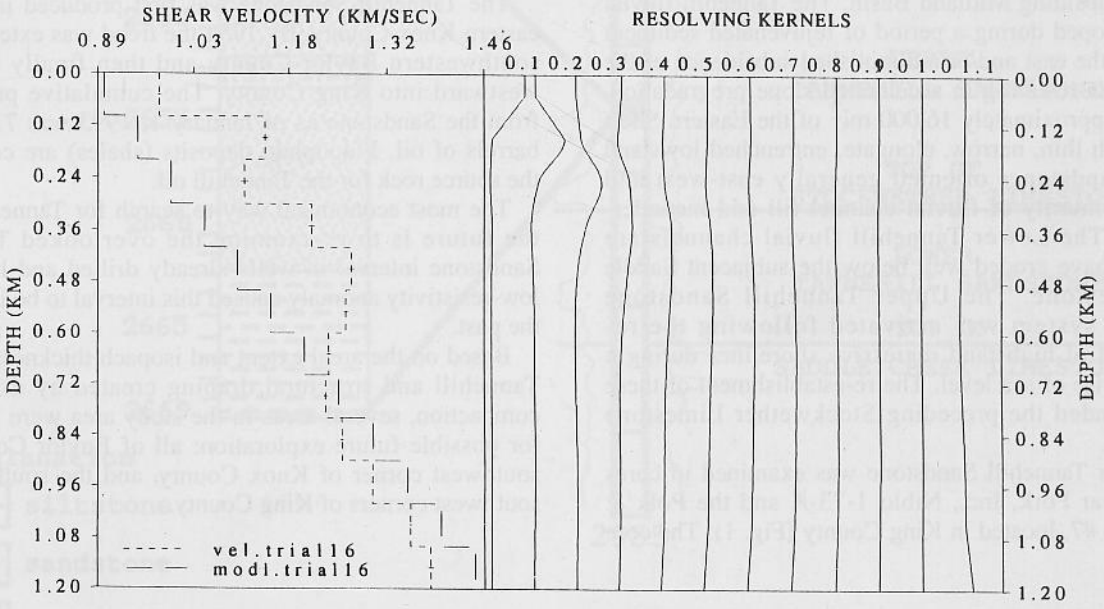

Fig. 2. Rayleigh wave inversion for shear velocity structure along Crawford path. Modl.trial16 represents an input start model that had layers of 0.10 km thickness increasing with depth at a constant rate. Vel.trial16 is the decoupled, non-causal model produced by the inversion of the dispersed Rayleigh waves along the Crawford path. Also shown are the resolving kernels, which show the ability of the model to resolve the layers in the earth's crust.

Subsurface Geology of the Permian Tannehill Sandstone in King, Knox, and Baylor Counties, North-Central Texas

Gary W. Crowe

The purpose of this study was to gain a better understanding of the Permian Tannehill Sandstone in the subsurface of King, Knox, and Baylor Counties. This included the areal extent, thickness, and pattern of Tannehill Sandstone deposits.

The study area is located in the southwestern third of Baylor County and the southern halves of Knox and King Counties in north-central Texas. These counties are located in the northern portion of the Eastern Shelf and east of the Concho Arch and Midland Basin. The Electra Arch and Wichita Thrust System are located to the northeast and the Bend Flexure, Fort Worth Basin, and the Ouachita Fold Belt are located east of the study area. The Tannehill Sandstone is located stratigraphically between the base of the Dothan Limestone and the top of the Saddle Creek Limestone of the Pueblo Formation, Cisco Group, Wolfcampian Series and the Permian System. It is divided into Lower and Upper Tannehill Sandstone units by the Stockwether Limestone (Figs. 1, 2).

The Tannehill Sandstone was deposited as point bars in a fluvial system that shifted back and forth, depositing its load across a relatively flat (<1°) Eastern Shelf westward toward the subsiding Midland Basin. The Tannehill fluvial system developed during a period of rejuvenated sediment supply from the east and/or a diminished subsidence of the Midland Basin resulting in accelerated slope progradation. Regionally, approximately 16,000 mi^2 of the Eastern Shelf are laced with thin, narrow, elongate, entrenched lowstand Tannehill Sandstones oriented generally east-west and composed primarily of fluvial channel-fill and meander-belt facies. The Lower Tannehill fluvial channels are observed to have eroded well below the subjacent Saddle Creek Limestone. The Upper Tannehill Sandstone terrigenous system was activated following the re-establishment of highstand regressive shorelines during a late relative rise of sea level. The re-establishment of these shorelines ended the preceding Stockwether Limestone transgression.

The Lower Tannehill Sandstone was examined in cores from the Clear Fork, Inc., Niblo 1-73-A and the Polk & Patton, Niblo #7, located in King County (Fig. 1). The core shows a fining-upward sequence and cross beds characteristic of a point bar. The Upper Tannehill Sandstone was examined in a core from the Taubert, Steed, Gunn and Medders UUU-7, located in eastern King County (Fig. 2). It also shows the characteristic upwardfining sequence and cross beds. The Lower Tannehill Sandstone, where present, has a thickness of up to 100 feet and the Upper Tannehill Sandstone has a thickness of up to 75 feet.

Tannehill hydrocarbons are trapped both stratigraphically and structurally in the study area. The hydrocarbons are trapped against the updip porosity pinchouts created by the floodplain shales. The stratigraphic traps are accentuated structurally by differential compaction of floodplain shales and channel-fill sand. Channel sands compact very little in comparison to shales, which can compact to 45%-55% of their original depositional thickness. The uneven distribution of sand and shale causes uneven compaction, creating structural draping. These structural drapes can be identified with the assistance of the structural map on the base of the Dothan Limestone. These drapes can help identify possible new exploration sites.

The Tannehill Sandstone was first produced in 1950 in eastern Knox County. By 1954 the trend was extended into southwestern Baylor County and then finally extended westward into King County. The cumulative production from the Sandstone as of January 1, 1993 was 73,657,196 barrels of oil. Floodplain deposits (shales) are considered the source rock for the Tannehill oil.

The most economical way to search for Tannehill oil in the future is to re-examine the overlooked Tannehill Sandstone interval in wells already drilled and logged. A low-resistivity anomaly caused this interval to be ignored in the past.

Based on the areal extent and isopach thicknesses of the Tannehill and structural draping created by differential compaction, several areas in the study area were identified for possible future exploration: all of Baylor County, the southwest corner of Knox County, and the southeast and southwest corners of King County.

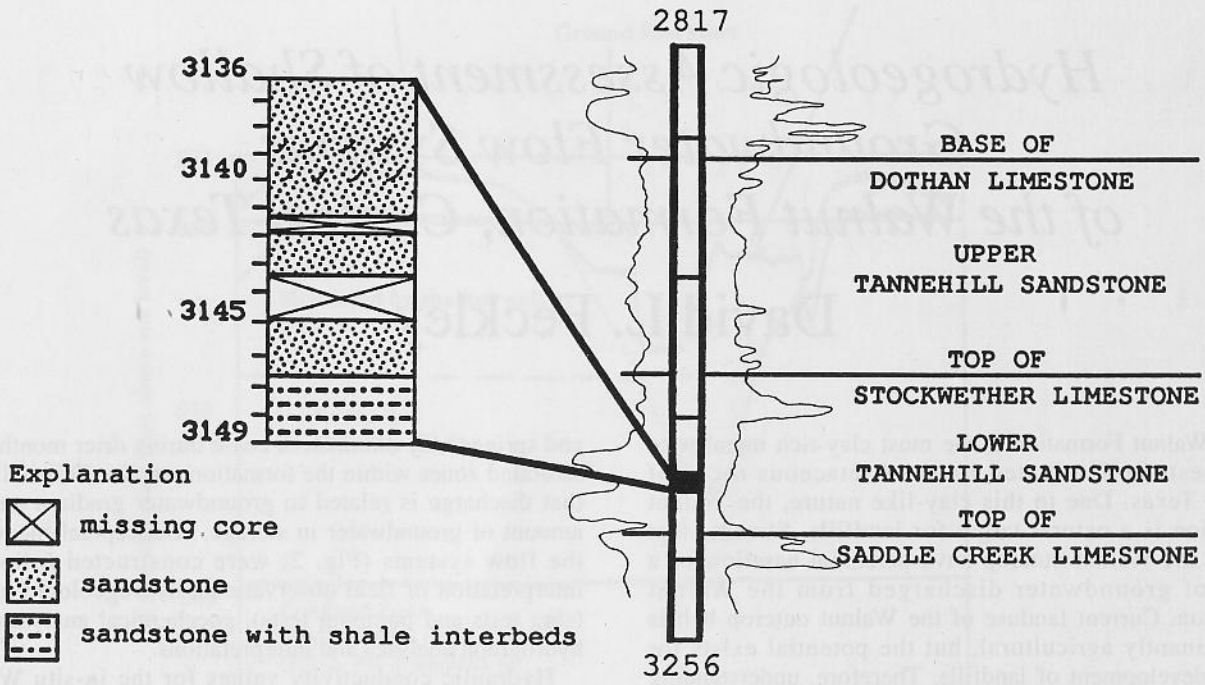

Fig. 1. Diagram showing graphically the characteristics of the Tannehill Sandstone in the Clear Fork, Inc., Niblo No. 1-73-A, located in central King County. As shown on the electric log, the Niblo No. 1-73-A core represents the Lower Tannehill Sandstone. Numbers on core log are feet below surface.

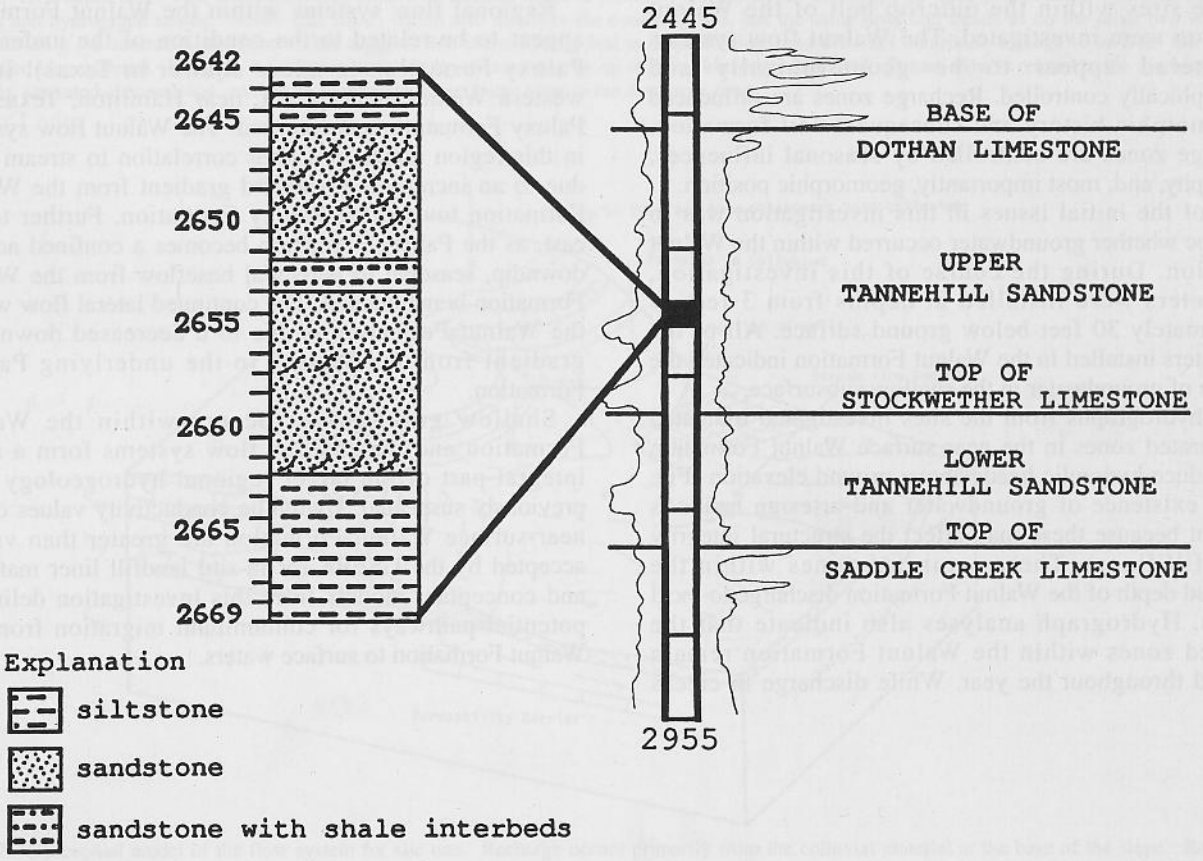

Fig. 2. Diagram showing graphically the characteristics of the Tannehill Sandstone in the Taubert, Steed, Gunn and Medders No. UUU-7, located in eastern King County. As shown on the electric log, the UUU-7 core represents the Upper Tannehill Sandstone. Numbers on core log are feet below surface.

Hydrogeologic Assessment of Shallow Groundwater Flow Systems of the Walnut Formation, Central Texas

David L. Feckley

The Walnut Formation is the most clay-rich member of the limestone-dominated Lower Cretaceous rocks of Central Texas. Due to this clay-like nature, the Walnut Formation is a natural target for landfills. Streams that transect the Walnut outcrop have perennial baseflow as a result of groundwater discharged from the Walnut Formation. Current landuse of the Walnut outcrop belt is predominantly agricultural, but the potential exists for further development of landfills. Therefore, understanding groundwater flow systems in the Walnut Formation and their relationship to stream flow will help protect surface water quality and potential drinking water from contaminants. The area of investigation is limited to a portion of the outcrop belt that extends eastward from Hamilton to Walnut Springs, and northward from Killeen to Weatherford, Texas.

Three sites within the outcrop belt of the Walnut Formation were investigated. The Walnut flow systems encountered appear to be geomorphically and stratigraphically controlled. Recharge zones are influenced by geomorphic history and subsequent soil formation. Discharge zones are controlled by seasonal influences, stratigraphy, and, most importantly, geomorphic position.

One of the initial issues in this investigation was to determine whether groundwater occurred within the Walnut Formation. During the course of this investigation, piezometers were installed at depths from 3 feet to approximately 30 feet below ground surface. All of the piezometers installed in the Walnut Formation indicated the presence of groundwater in the shallow subsurface.

Well hydrographs from the sites investigated indicated that saturated zones in the near surface Walnut Formation may produce hydraulic heads above ground elevation (Fig. 1). The existence of groundwater and artesian heads is important because these may affect the structural integrity of landfill liners. These saturated zones within the weathered depth of the Walnut Formation discharge to local streams. Hydrograph analyses also indicate that the saturated zones within the Walnut Formation remain saturated throughout the year. While discharge to creeks and springs may diminish or cease during drier months, the saturated zones within the formation remain. This indicates that discharge is related to groundwater gradient and the amount of groundwater in storage. Conceptual models of the flow systems (Fig. 2) were constructed following interpretation of field observations, hydrogeologic testing (slug tests and pumping tests), goechemical analyses, and hydrograph analyses and interpretations.

Hydraulic conductivity values for the in-situ Walnut material at the sites tested ranged from 3.5 x 100^{-6} cm/sec to 2.5 x 10^{-4} cm/sec. The results of the aquifer testing indicated that the in-situ Walnut Formation possessed hydraulic conductivity values greater than the maximum hydraulic conductivity allowed by the United States Environmental Protection Agency (USEPA) for in-situ landfill liners (10^{-7} cm/sec).

Regional flow systems within the Walnut Formation appear to be related to the condition of the underlying Paluxy Formation (a minor aquifer in Texas). In the western Walnut outcrop belt, near Hamilton, Texas, the Paluxy Formation is unconfined. The Walnut flow systems in this region maintain a poor correlation to stream flow due to an increased downward gradient from the Walnut Formation toward the Paluxy Formation. Further to the east, as the Paluxy Formation becomes a confined aquifer downdip, seasonal to perennial baseflow from the Walnut Formation is maintained. The continued lateral flow within the Walnut Formation is due to a decreased downward gradient from the Walnut to the underlying Paluxy Formation.

Shallow groundwater occurs within the Walnut Formation and the shallow flow systems form a more integral part of the larger regional hydrogeology than previously suspected. Hydraulic conductivity values of the near-surface Walnut Formation are greater than values accepted by the USEPA for in-situ landfill liner material, and conceptual models from this investigation delineate potential pathways for contaminant migration from the Walnut Formation to surface waters.

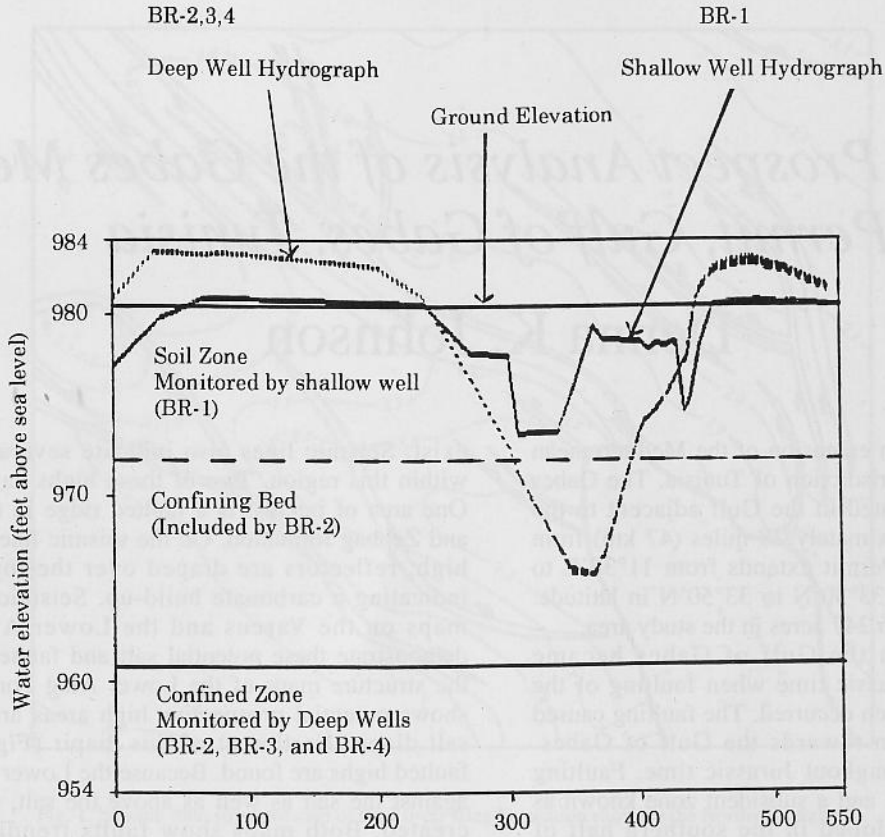

Fig. 1. System hydrograph from site one indicating the zones monitored and the water levels recorded from the wells. A shallow saturated soil zone exists from the ground surface to a depth of approximately 8 feet. This zone is monitored by BR-1. A confining bed for the deeper saturated clay interval is present beneath the soil zone from a depth of 8 feet to a depth of approximately 19 feet. The confining bed interval is included in the screened interval of BR-2. At a depth of 19 feet, a saturated clay zone with artesian heads is present. This zone was monitored by three piezometers, which all show similar heads and hydrograph trends. Notice that BR-2, which also monitors the confining bed, has the same head and trends as do the other two wells, which monitor only the saturated clay zone. This suggests that the confining bed is quite efficient, and does not contribute leakage to or from the underlying saturated clay material. Heads in the deeper confined clay system may be up to 3 feet above ground level. Stream flow is related to the discharge from the deeper, saturated clay material, and the gradient from the recharge zone to the discharge zone.

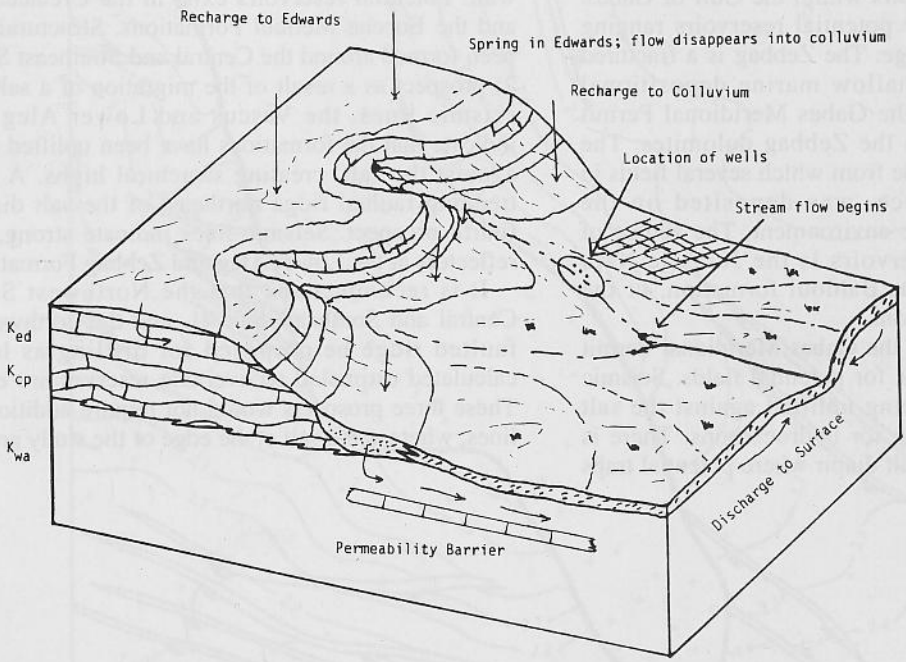

Fig. 2. Conceptual model of the flow system for site one. Recharge occurs primarily from the colluvial material at the base of the slope. Recharge that occurs within the Edwards Formation is discharged from springs located in the Edwards. This spring flow continues down the slope, and eventually disappears into the colluvial material. Water migrates vertically through the weathered Walnut, and migrates laterally when permeability barriers are encountered. Discharge to streams occurs when sufficient head, gradient, and geomorphic evolution cause the saturated zone to intersect the ground surface downstream (downgradient) of the well field.

A Petroleum Prospect Analysis of the Gabes Meridional Permit, Gulf of Gabes, Tunisia

Denna K. Johnson

The Gulf of Gabes is an extension of the Mediterranean Sea within the political jurisdiction of Tunisia. The Gabes Meridional Permit is located in the Gulf adjacent to the Libyan frontier and approximately 28 miles (47 km) from the Tunisian coast. The Permit extends from 11°30'E to 11°50'E in longitude and 33°30'N to 33°50'N in latitude. There are approximately 56,247 acres in the study area.

Structural activity in the Gulf of Gabes became prominent during the Triassic time when faulting of the southern Tunisia Dahar Arch occurred. The faulting caused sedimentation deposition towards the Gulf of Gabes. Subsidence occurred throughout Jurassic time. Faulting continued during this time and a subsident zone known as the Jeffara flexure developed in the southern half of Tunisia. One of the major structural developments in Tunisia was the North-South Axis. This axis started forming during Jurassic time and continued developing throughout the Paleocene, dividing western and eastern Tunisia. Throughout the Eocene, faulting and folding occurred in once-stable eastern Tunisia. Salt migration became activated at this time as well. The Gabes Meridional Permit has a major fault system that trends northwest-southeast.

The Cretaceous Zebbag and the Eocene Metloui are the two primary potential reservoirs within the Gulf of Gabes. There are several secondary potential reservoirs ranging from Jurassic to Eocene in age. The Zebbag is a fractured dolomite deposited in a shallow marine depositional environment. Wells within the Gabes Meridional Permit have hydrocarbon shows in the Zebbag dolomites. The Metloui, a bioclastic limestone from which several fields in the Gulf of Gabes produce, was deposited on the continental shelf of a marine environment. The source of hydrocarbons in these reservoirs is the Jurassic Nara Group, the upper Cretaceous Bahloul formation, or the Eocene Bou Dabbous formation.

Several salt diapirs within the Gabes Meridional Permit provide various types of traps for potential fields. Seismic lines indicate formations being uplifted against the salt edge, indicating an ideal trap for hydrocarbons. There is complex faulting above the salt diapir where potential traps exist. Seismic lines also indicate several faulted highs within this region. Two of these highs have been drilled. One area of interest is a faulted ridge in the Lower Aleg and Zebbag formation. On the seismic line that shows this high, reflectors are draped over the top of the ridge, indicating a carbonate build-up. Seismic time structure maps on the Vascus and the Lower Aleg Formation demonstrate these potential salt and faulted traps. One of the structure maps of the Lower Aleg Formation (Fig. 1) shows potential prospective high areas around most of a salt diapir. Northwest of this diapir (Fig. 2) additional faulted highs are found. Because the Lower Aleg is uplifted against the salt as well as above the salt, traps have been created. Both maps show faults trending northwest-southeast, corresponding to the regional trend.

There are four areas with hydrocarbon potential, three of which are surrounding salt diapirs. One potential prospect area surrounding salt is near the edge of the study area; additional seismic lines would be needed for a better understanding of the area. Two of the prospects are involved with the same salt diapir but at different locations (Figs. 1, 2). The Northwest Salt #1 prospect (Fig. 1) has structural traps developed as a result of a northwest-southeast trending graben and a similar trending salt diapir wall. Potential reservoirs exist in the Cretaceous Zebbag and the Eocene Metloui Formations. Structural traps have been formed around the Central and Southeast Salt #1 (Fig. 2) prospect as a result of the migration of a salt diapir. On seismic lines, the Vascus and Lower Aleg reflectors indicate that the formations have been uplifted and pushed against the salt, creating structural highs. A northwest-trending faulted ridge northeast of the salt diapirs is the fourth prospect. Seismic lines indicate strong, horizontal reflectors at the Lower Aleg and Zebbag Formations.

It is recommended that the Northwest Salt #1, the Central and Southeast Salt #1, and the northwest-trending faulted ridge be proposed for drilling as long as the calculated estimated recoverable reserves are economical. These three prospects would not require additional seismic lines, whereas the salt at the edge of the study area would.

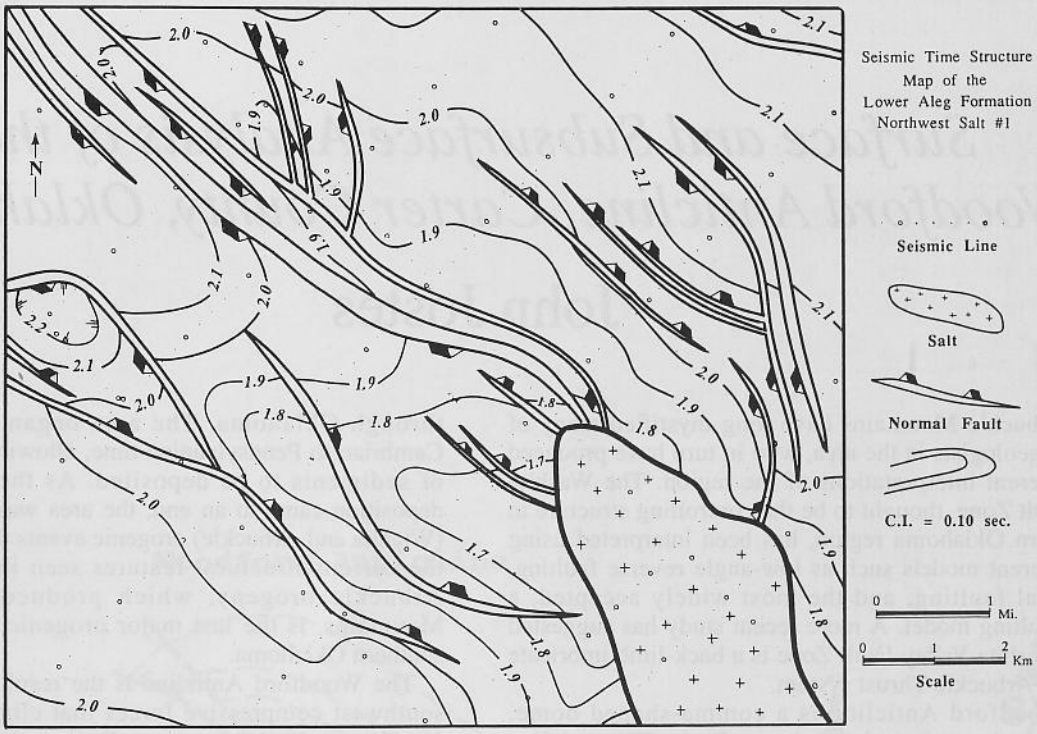

Fig. 1. Seismic time structure map of the Lower Aleg Formation showing the Northwest Salt #1.

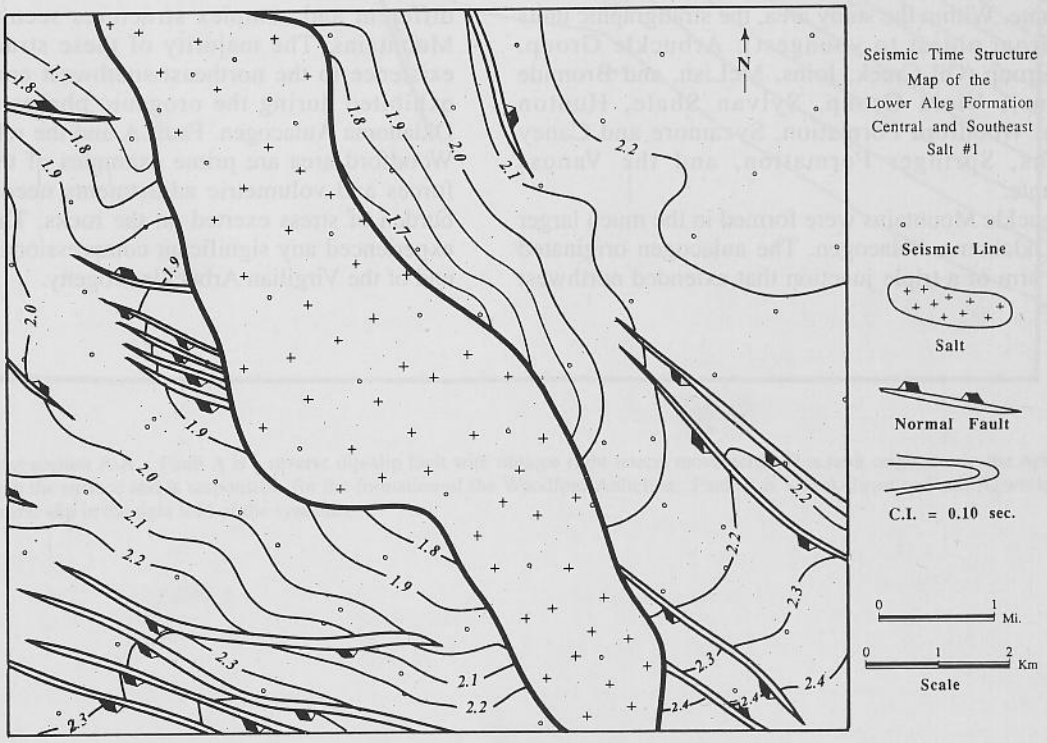

Fig. 2. Seismic time structure map of the Lower Aleg Formation showing the Central and Southeast Salt #1.

Surface and Subsurface Analysis of the Woodford Anticline, Carter County, Oklahoma

John Jostes

The Arbuckle Mountains have long mystified many of the finest geologists in the area, who in turn have produced many different interpretations of the region. The Washita Valley Fault Zone, thought to be the controlling structure in the southern Oklahoma region, has been interpreted using many different models such as low-angle reverse faulting, extensional faulting, and the most widely accepted, a wrench-faulting model. A more recent study has suggested that the Washita Valley Fault Zone is a back-limb imbricate of a larger Arbuckle Thrust system.

The Woodford Anticline is a comma-shaped dome, plunging southwest into the Ardmore Basin. The anticline is located on the southwestern flank of the Arbuckle Mountains, approximately nine miles northwest of the town of Ardmore, Oklahoma. The Washita Valley Fault strikes N.60°W. and is located to the north of the study area, while the Ardmore Basin lays to the south. An understanding of the whole Arbuckle Mountain region, and Woodford Anticline in particular, will provide a better perspective for the development of the southwestern flank of the Arbuckle Mountains.

The stratigraphy within southern Oklahoma ranges from Precambrian granites to the Pennsylvanian Vanoss Conglomerate. Within the study area, the stratigraphic units include (from oldest to youngest): Arbuckle Group, Simpson Group (Oil Creek, Joins, McLish, and Bromide Formations), Viola Group, Sylvan Shale, Hunton Formation, Woodford Formation, Sycamore and Caney Formations, Springer Formation, and the Vanoss Conglomerate.

The Arbuckle Mountains were formed in the much larger Southern Oklahoma Aulacogen. The aulacogen originated as a failed arm of a triple junction that extended northwest through Oklahoma. The area began to subside from Cambrian to Pennsylvanian time, allowing thick sequences of sediments to be deposited. As the subsidence and deposition came to an end, the area was subjected to two (Wichita and Arbuckle) orogenic events that would produce the current structural features seen in Oklahoma. The Arbuckle orogeny, which produced the Arbuckle Mountains, is the last major orogenic episode to affect southern Oklahoma.

The Woodford Anticline is the result of the northeast-southwest compressive forces that climaxed in the Late Virgilian Arbuckle orogeny. During this time, Paleozoic rocks were thrust to the southwest on the northeast-dipping Washita Valley Fault. With continued compression, Fault A developed, forming the Woodford Anticline (Fig 1). Fault A is a reverse dip-slip fault with oblique right-lateral slip. Volumetric adjustments produced by the faulting resulted in the formation of numerous faults on the hanging wall (east fault block) and footwall (west fault block). Many of the volumetric adjustment faults are generated as bedding plane faults along the detachment horizons in the Oil Creek, McLish, and Woodford Formations.

The Woodford Anticline is one example of the many different and complex structures seen in the Arbuckle Mountains. The majority of these structures owe their existence to the northeast-southwest compressive forces exhibited during the orogenic phases of the Southern Oklahoma Aulacogen. Fault A and the related faults in the Woodford area are prime examples of these compressive forces and volumetric adjustments needed to relieve the burden of stress exerted on the rocks. This region has not experienced any significant compressional forces since the end of the Virgilian Arbuckle orogeny.

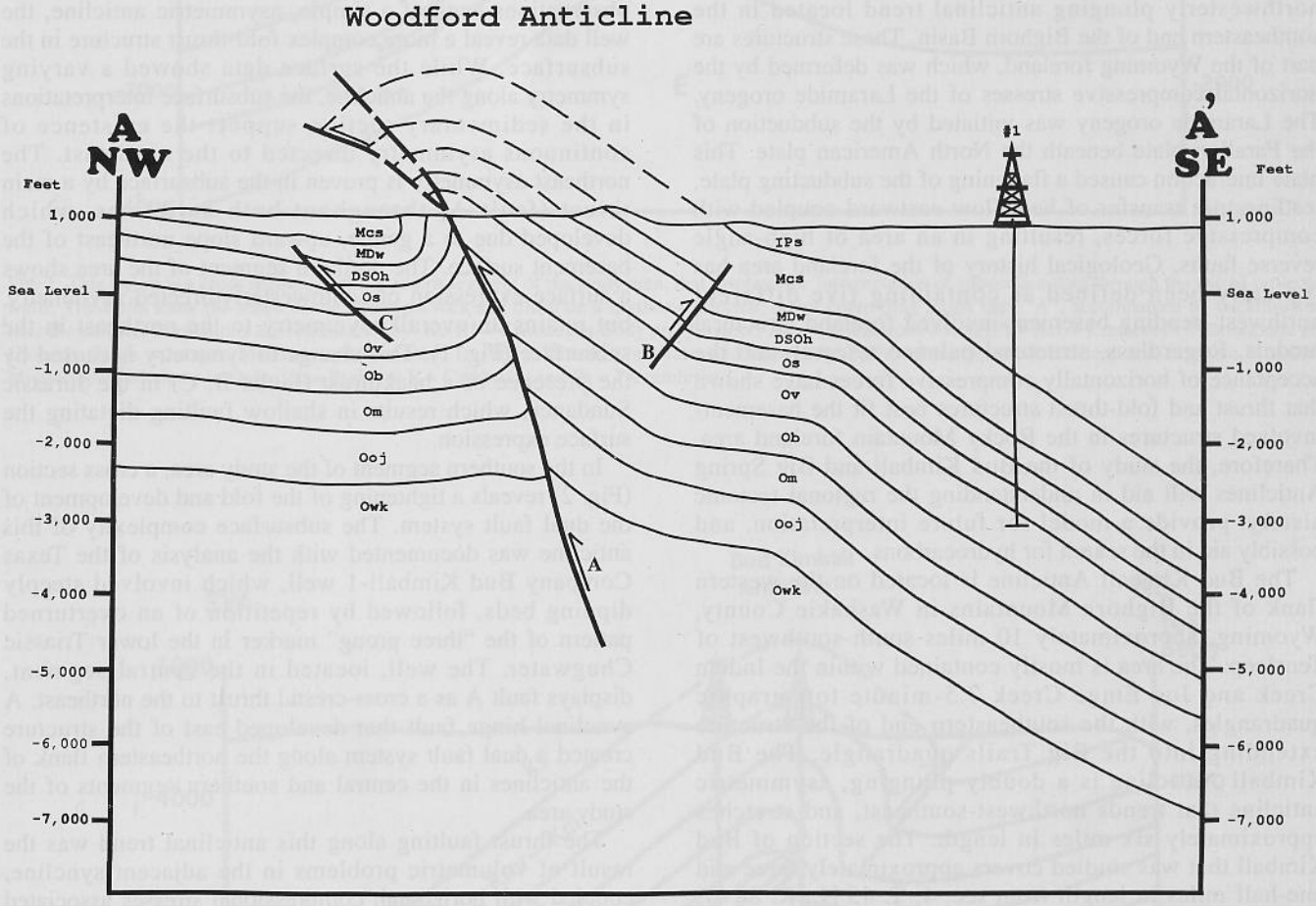

Fig. 1. NW to SE cross section A-A´. Fault A is a reverse dip-slip fault with oblique right-lateral movement. This fault originates in the Arbuckle Group (Owk) and cuts through the surface and is responsible for the formation of the Woodford Anticline. Fault B is a back-thrust to Fault A, while Fault C is a thrust fault due to flexural slip in the tight fold of the syncline.

Structural Geology of the Bud Kimball and Big Spring Anticlines, Southern Bighorn Basin, Washakie County, Wyoming

Scott M . Krauszer

The Bud Kimball and Big Spring Anticlines are part of a northwesterly plunging anticlinal trend located in the southeastern end of the Bighorn Basin. These structures are part of the Wyoming foreland, which was deformed by the horizontal compressive stresses of the Laramide orogeny. The Laramide orogeny was initiated by the subduction of the Farallon plate beneath the North American plate. This plate interaction caused a flattening of the subducting plate, leading to a transfer of heat flow eastward coupled with compressive forces, resulting in an area of high-angle reverse faults. Geological history of the foreland area has typically been defined as containing five different northwest-trending basement-involved foreland structural models. Regardless, structural balance research and the acceptance of horizontally compressive forces have shown that thrust and fold-thrust structures best fit the basement-involved structures in the Rocky Mountain foreland area. Therefore, the study of the Bud Kimball and Big Spring Anticlines will aid in understanding the regional tectonic history, provide a model for future interpretation, and possibly aid in the search for hydrocarbons.

The Bud Kimball Anticline is located on the western flank of the Bighorn Mountains in Washakie County, Wyoming, approximately 10 miles south-southwest of Tensleep. The area is mostly contained within the Indian Creek and Joe Emge Creek 7.5-minute topographic quadrangles, with the southeastern end of the structure extending into the Big Trails quadrangle. The Bud Kimball Anticline is a doubly plunging, asymmetric anticline that trends northwest-southeast, and stretches approximately six miles in length. The section of Bud Kimball that was studied covers approximately three and one-half miles in length from sec. 4, T. 45 N., R. 88 W, southeast to sec. 14, T. 45 N., R. 88 W., and two miles in width. The southernmost end of Bud Kimball Anticline plunges southeast, into the Big Spring Anticline. The Big Spring Anticline plunges northwesterly and continues for approximately eleven miles, following the same trend as Bud Kimball Anticline. The part of the Big Spring Anticline that was studied includes the northwestern plunge-end in sec. 14, T. 45 N., R. 88 W., continuing southwest to the eastern border of sec. 31, T. 45 N., R. 87 W.

Although the surface expression and seismic observations suggest a simple, asymmetric anticline, the well data reveal a more complex fold-thrust structure in the subsurface. While the surface data showed a varying symmetry along the anticline, the subsurface interpretations in the sedimentary section support the existence of continuous asymmetry directed to the northeast. The northeast asymmetry is proven in the subsurface by a main thrust (fault A) throughout both anticlines, which developed due to a gentle, upward slope northeast of the basement surface. The northern segment of the area shows a surface expression of southwesterlydirected asymmetry, but retains an overall asymmetry to the northeast in the subsurface (Fig. 1). This change in symmetry is caused by the presence of a backthrust (faults B, C) in the Jurassic Sundance, which results in shallow faulting dictating the surface expression.

In the southern segment of the study area, a cross section (Fig. 2) reveals a tightening of the fold and development of the dual fault system. The subsurface complexity of this anticline was documented with the analysis of the Texas Company Bud Kimball-1 well, which involved steeply dipping beds, followed by repetition of an overturned pattern of the "three prong" marker in the lower Triassic Chugwater. The well, located in the central segment, displays fault A as a cross-crestal thrust to the northeast. A synclinal hinge fault that developed east of the structure created a dual fault system along the northeastern flank of the anticlines in the central and southern segments of the study area.

The thrust faulting along this anticlinal trend was the result of volumetric problems in the adjacent syncline, coupled with horizontal, compressional stresses associated with the Laramide orogeny. This supports structural interpretations that follow the basic style of Wyoming foreland deformation, and provides a model for future structural interpretation of the Bighorn basin area. In addition, the subsurface interpretations could aid in the future search for hydrocarbons by revealing possible structural traps associated with the thrusting and deformation in the Bighorn basin area.

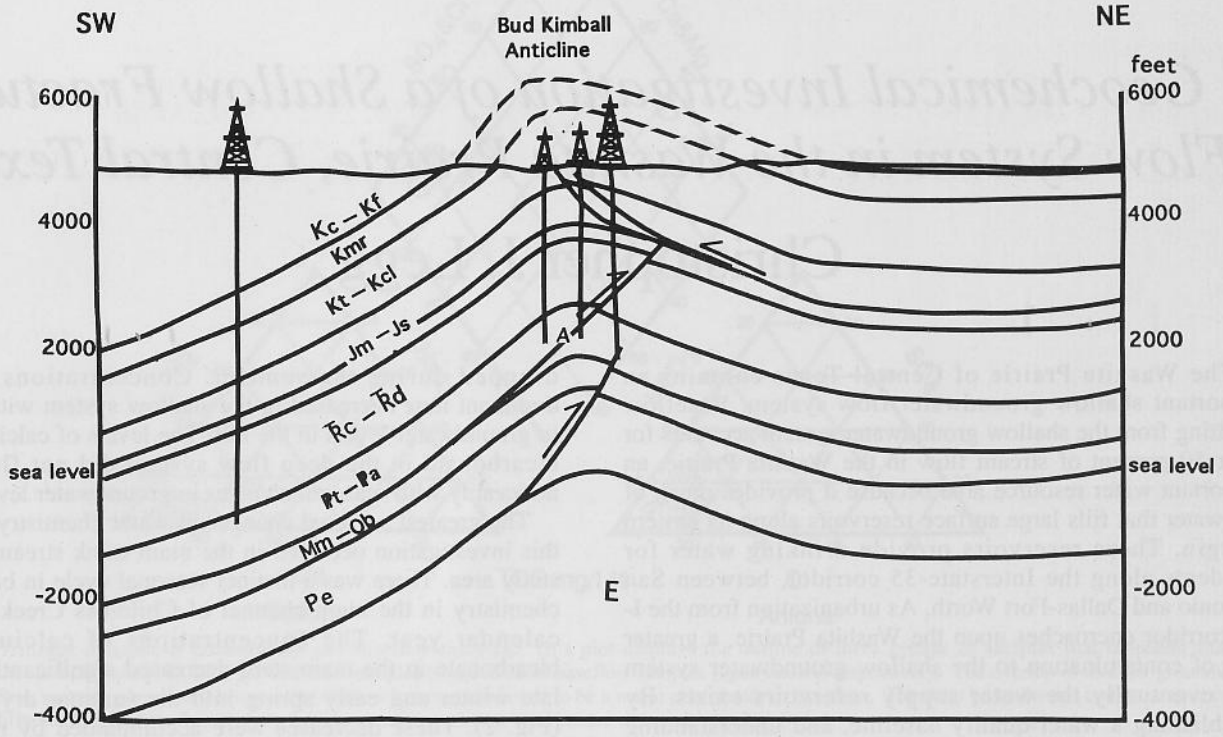

Fig. 1. This figure is a cross section, in the northern segment of the study area, that displays the interpretation of subsurface data through the use of projected wells. The wells show the shape of the basement rock and illustrate a northeast-directed, major controlling thrust fault "A", accompanied by backthrusting near the surface. Formations are represented by: Kc-Kf = Cretaceous Cody and Frontier; Kmr = Cretaceous Mowry; Kt-Kcl = Cretaceous Thermopolis and Cloverly; Jm-Js = Jurassic Morrison and Sundance; Trc-Trd = Triassic Chugwater and Dinwoody; Pt-Pa = Pennsylvanian Tensleep and Amsden; Mm-Ob = Mississippian Madison to Ordovician Bighorn; E = Cambrian; and Pe = Precambrian.

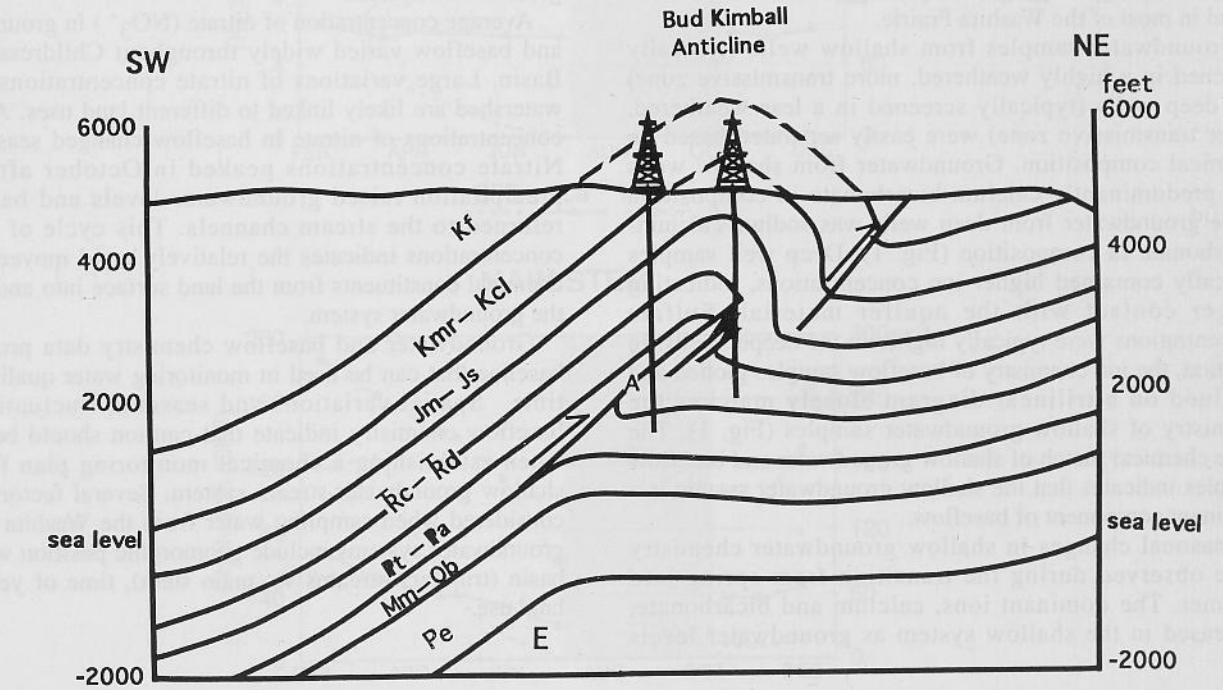

Fig. 2. This figure displays a cross section, in the south-central segment of the study area, that is interpreted in the subsurface as a dual fault system, coupled with complex folding defined by well data along the line of section. The major controlling thrust fault "A" continues throughout the study area. Formations are represented by: Kf = Cretaceous Frontier; Kmr-Kcl = Cretaceous Mowry and Cloverly; Jm-Js = Jurassic Morrison and Sundance; Trc-Trd = Triassic Chugwater and Dinwoody; Pt-Pa = Pennsylvanian Tensleep and Amsden; Mm-Ob = Mississippian Madison to Ordovician Bighorn; E = Cambrian; and Pe = Precambrian.

A Geochemical Investigation of a Shallow Fracture-Flow System in the Washita Prairie, Central Texas

Christopher J. Legg

The Washita Prairie of Central Texas contains an important shallow groundwater flow system. Baseflow emitting from the shallow groundwater system accounts for over 50 percent of stream flow in the Washita Prairie, an important water resource area because it provides much of the water that fills large surface reservoirs along its eastern margin. These reservoirs provide drinking water for residents along the Interstate-35 corridor, between San Antonio and Dallas-Fort Worth. As urbanization from the I-35 corridor encroaches upon the Washita Prairie, a greater risk of contamination to the shallow groundwater system and eventually the water supply reservoirs exists. By establishing a water-quality baseline, and understanding seasonal trends in baseflow and groundwater chemistry, future monitoring and management of this system will be improved.

This investigation evaluated the chemistry of groundwater and baseflow in Childress Creek Basin over the seasonal fluctuations of calendar year 1993. Childress Creek Basin was selected for study because it occupies a large area (approximately 80 square miles) of the Washita Prairie and is similar to other large expanses of limestone terrain in Central Texas. The watershed contains representative geology, geomorphology, soils, and land use found in most of the Washita Prairie.

Groundwater samples from shallow wells (typically screened in a highly weathered, more transmissive zone) and deep wells (typically screened in a less weathered, lower transmissive zone) were easily separated based on chemical composition. Groundwater from shallow wells was predominantly calcium-bicarbonate in composition while groundwater from deep wells was sodium-calcium-bicarbonate in composition (Fig. 1). Deep well samples typically contained higher ion concentrations, indicating longer contact with the aquifer material. Sulfate concentrations were typically higher in the deeper wells. In addition, the ion chemistry of baseflow samples plotted and outlined on a trilinear diagram closely matches the chemistry of shallow groundwater samples (Fig. 1). The close chemical match of shallow groundwater and baseflow samples indicates that the shallow groundwater system is a dominant component of baseflow.

Seasonal changes in shallow groundwater chemistry were observed during the transition from spring into summer. The dominant ions, calcium and bicarbonate, increased in the shallow system as groundwater levels dropped during the summer. Concentrations of the dominant ions decreased in the shallow system with a rise in groundwater levels in the fall. The levels of calcium and bicarbonate in the deep flow system did not fluctuate noticeably with seasonal changes in groundwater levels.

The greatest seasonal changes in water chemistry during this investigation occurred in the main trunk stream of the study area. There was a distinct seasonal cycle in baseflow chemistry in the main channel of Childress Creek over a calendar year. The concentrations of calcium and bicarbonate in the main stem decreased significantly from late winter and early spring into the summer dry period (Fig. 2). These decreases were accompanied by reduced CO_2 partial pressures in baseflow. Concentrations of the major ions rose in the fall recharge period.

While there were significant changes in major ion concentrations in the main trunk stream of the study area, ion concentrations in the tributaries of Childress Creek remained relatively consistent through seasonal fluctuations in baseflow discharge (Fig. 2). After the summer dry period the major ion concentrations were nearly the same as concentrations before the stream dried up. Consistent chemistry of baseflow is characteristic of a diffuse-flow groundwater system.

Average concentration of nitrate (NO_3^-) in groundwater and baseflow varied widely throughout Childress Creek Basin. Large variations of nitrate concentrations in the watershed are likely linked to different land uses. Average concentrations of nitrate in baseflow changed seasonally. Nitrate concentrations peaked in October after fall precipitation raised groundwater levels and baseflow returned to the stream channels. This cycle of nitrate concentrations indicates the relatively rapid movement of chemical constituents from the land surface into and out of the groundwater system.

Groundwater and baseflow chemistry data provide a baseline that can be used in monitoring water quality over time. Spatial variations and seasonal fluctuations in baseflow chemistry indicate that caution should be taken when establishing a chemical monitoring plan for this shallow groundwater-stream system. Several factors to be considered when sampling water from the Washita Prairie groundwater systems include geomorphic position within a basin (tributary streams vs. main stem), time of year, and land use.

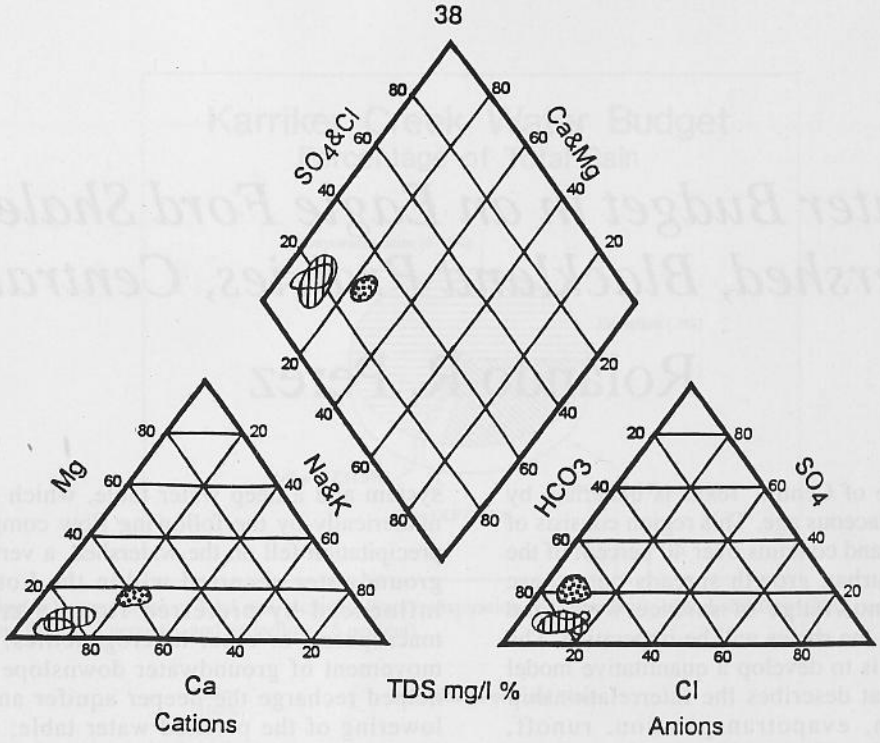

Fig. 1. Trilinear diagram of groundwater and baseflow samples. This plot displays the outline of three groups of samples that represent shallow groundwater samples (striped), deep groundwater samples (stippled), and baseflow samples (open circles) respectively. The overlap of shallow groundwater and baseflow samples is expected because the shallow system is believed to be a major contributor to baseflow. The deep groundwater system samples were slightly different from the shallow system, having a sodium-calcium-bicarbonate composition.

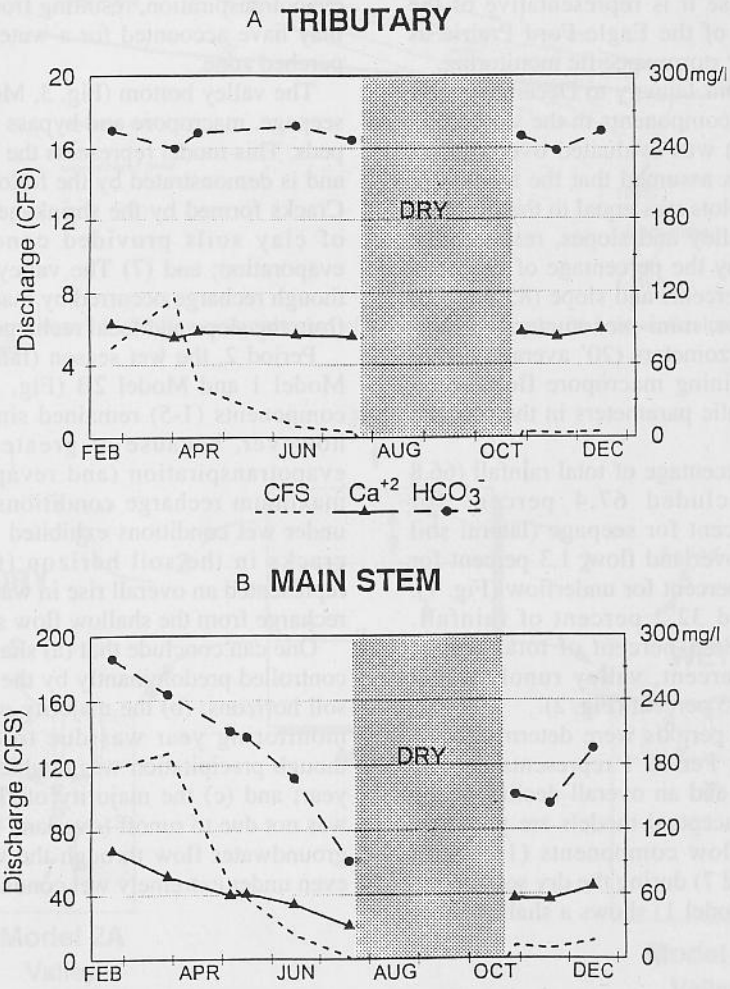

Fig. 2. Seasonal chemical variations of baseflow. The tributary hydrograph (A) is from baseflow station 5 on Eisenhower Creek and the mainstream hydrograph (B) is from baseflow station 1 located on Childress Creek. Both hydrographs have similar seasonal trends. Calcium and bicarbonate concentrations are relatively consistent in the tributary despite seasonal fluctuations in discharge. Calcium and bicarbonate concentrations in the main stem were not consistent, but decreased sharply with baseflow recession. With the return of baseflow in the fall, ion concentrations in the main stem were higher than in the early summer and continued to rise into the winter.

Water Budget in an Eagle Ford Shale Sub-Watershed, Blackland Prairies, Central Texas

Rolando R. Perez

The Blackland Prairie of Central Texas is underlain by chalks and shales of Cretaceous age. This region consists of about nine million acres and contains over 40 percent of the state's population. As urban growth spreads onto these shales, the need for knowledge of surface-water and groundwater flow within the shales will be imperative. The purpose of this research is to develop a quantitative model in a shale watershed that describes the interrelationship between precipitation, evapotranspiration, runoff, infiltration, lateral flow, deep flow, and baseflow.

A sub-watershed (dubbed Karriker Creek) located in the northwestern area of Bell Co., Texas, was chosen for an analysis of the water budget within the Eagle Ford Shale. The site was selected because it is representative of the typical soils and lithologies of the Eagle Ford Prairie as well as for its accessibility for storm-specific monitoring.

Seasonal measurements from January to December 1991 were used to determine flow components in the watershed. Total runoff (plots and weir) was evaluated over various soil groups and slopes. It was assumed that the amount of water flowing off the runoff plots was equal to the overland flow component from the valley and slopes, respectively. This quantity was weighted by the percentage of the basin occupied by the valley (15 percent) and slope (85 percent) terrains. Soil moisture blocks, mini-piezometers, shrink-swell rods, and four deep piezometers (20' average depth) were instrumental in determining macropore flow, water table fluctuations, and hydraulic parameters in the soil and weathered shales.

The water balance, as a percentage of total rainfall (66.8 inches for the year), included 67.4 percent for evapotranspiration, 28.2 percent for seepage (lateral soil flow), 2.6 percent for slope overland flow, 1.3 percent for valley overland flow, and .5 percent for underflow (Fig. 1). Total stream flow averaged 32.2 percent of rainfall. Groundwater seepage was 86.5 percent of total stream flow; slope runoff was 8 percent, valley runoff was 4 percent, and underflow was 1.5 percent (Fig. 2).

Two distinct water budget periods were determined for the monitoring year (Fig. 3). Period 1 represents the dry season (late spring, summer) and an overall decline in the regional water table. Two conceptual models are proposed in order to compare slope flow components (1-5) with valley flow components (6 and 7) during the dry season.

The upper slope (Fig. 3, Model 1) shows a shallow flow system and a deep water table, which can be illustrated numerically by the following flow components: (1) After precipitation fell on the watershed, a vertical movement of groundwater occurred within the Lott soils generally influenced by preferred flow in cracks, fractures, macropores, or other heterogeneities; (2) A horizontal movement of groundwater downslope (or lateral flow) helped recharge the deeper aquifer and resulted in the lowering of the perched water table; (3) Groundwater fluctuations within the slope represented a rising and falling water table due to recharge, discharge, and evaporation; (4) Flow from both the shallow flow system and the deeper water table, recharged the valley; and (5) Water loss by evapotranspiration, resulting from seepage and macropores, may have accounted for a water table drop in the shallow perched zone.

The valley bottom (Fig. 3, Model 2A) recharged through seepage, macropore and bypass flow, among widely spaced peds. This model represents the valley under dry conditions and is demonstrated by the following flow components: (6) Cracks formed by the shrinkage resulting from desiccation of clay soils provided conduits for water flow or evaporation; and (7) The valley water table dropped even though recharge occurred by macropore flow and deep flow from the slope and local recharge.

Period 2, the wet season (fall, winter) is represented by Model 1 and Model 2B (Fig. 3). In general, slope flow components (1-5) remained similar to those of Period 1; however, because of greater precipitation and less evapotranspiration (and revap), the system was under maximum recharge conditions. The valley (Model 2B) under wet conditions exhibited recharge primarily through cracks in the soil horizon (flow component 6), and represented an overall rise in water table conditions through recharge from the shallow flow system (flow component 7).

One can conclude that (a) shallow groundwater flow was controlled predominantly by the weathered shale zones and soil horizons; (b) the majority of total consumption for the monitoring year was due to evapotranspiration, even though precipitation was double that of an average rainfall year; and (c) the majority of flow through the watershed was not due to runoff (overland flow), but rather to shallow groundwater flow through the weathered shales and soils, even under extremely wet conditions.

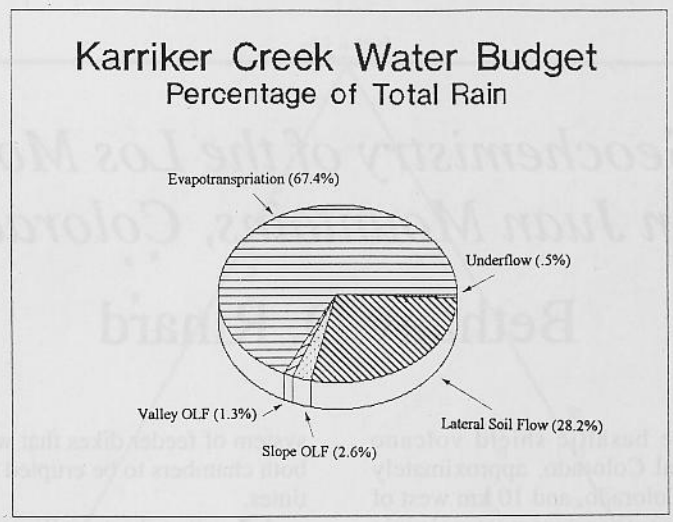

Fig. 1. The water budget as a percentage of total rain included evapotranspiration (67.4 percent), lateral soil flow (28.2 percent), slope overland flow (2.6 percent), valley overland flow (1.3 percent), and underflow (.5 percent).

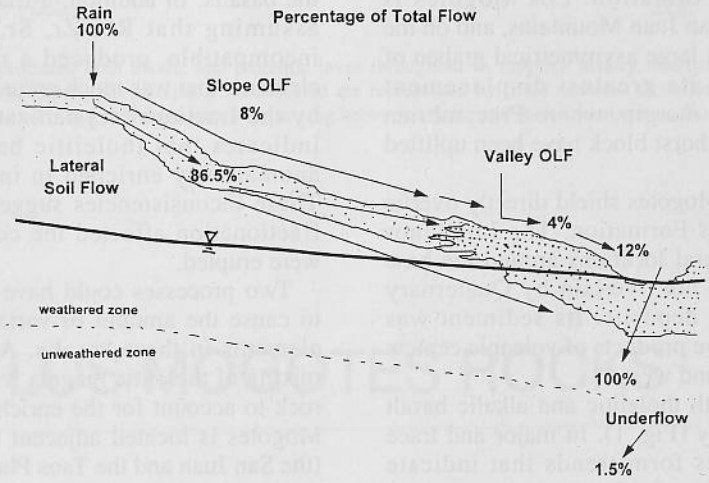

Fig. 2. The water budget as a percentage of total flow was composed of groundwater seepage (86.5 percent), slope runoff (8 percent), valley runoff (4 percent), and underflow (1.5 percent).

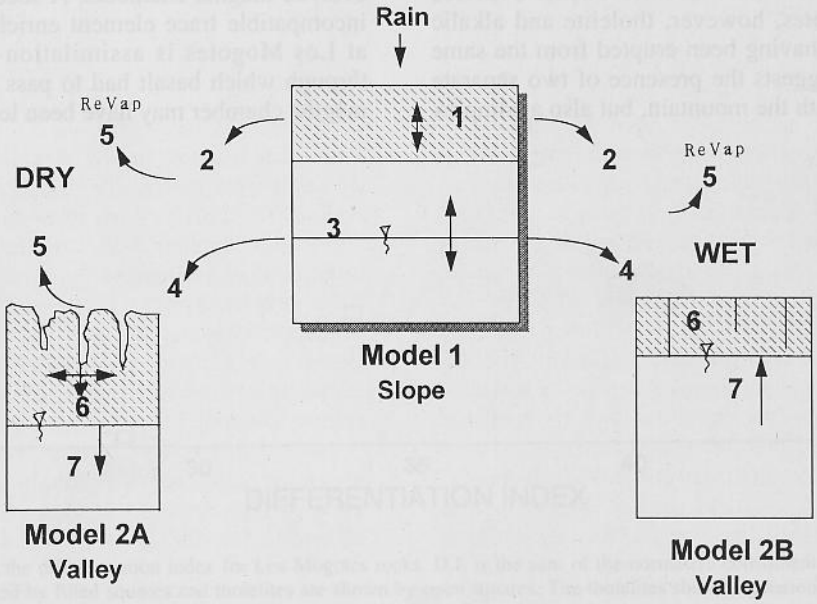

Fig. 3. Two distinct periods in developing models for a dry and wet season on an Eagle Ford Shale sub-watershed were determined. Period 1 (left diagram) represents the dry season with an overall decline in water table elevation. Model 1 demonstrates discharge by lateral flow in the slope, whereas Model 2A shows recharge through macropores. Revap (seepage evaporation and evapotranspiration) accounts for a high water loss. Period 2 (right diagram) represents the wet season with a rising water table. Model 1 is under maximum saturated conditions during this period. Flow components (1-7) represent: infiltration, lateral flow, the potentiometric surface, shallow flow, macropore flow, and the overall water table trends (respectively).

Geology and Geochemistry of the Los Mogotes Volcano, San Juan Mountains, Colorado

Bethany D. Rinard

Los Mogotes is a Pliocene basaltic shield volcano located in extreme south-central Colorado, approximately 50 km southwest of Alamosa, Colorado, and 10 km west of Antonito, Colorado. It is the southeasternmost volcanic center within the San Juan Volcanic Field, and the youngest eruptive center for the Hinsdale Basalt, the most extensive member of the Hinsdale Formation. Los Mogotes is bounded on the west by the San Juan Mountains, and on the east by the San Luis Valley, a large asymmetrical graben of the Rio Grande rift, with its greatest displacement occurring along the eastern margin, where Precambrian rocks of the Sangre de Cristo horst block have been uplifted along a major normal fault.

Basaltic lavas of the Los Mogotes shield directly overlie the volcaniclastic Los Pinos Formation. The Los Pinos Formation is exposed at several locations around the base of the mountain where it is not overlain by Quaternary alluvial or glacial outwash deposits. Its sediment was derived from the older eruptive products of volcanic centers in the San Juans to the north and west.

Los Mogotes produced both tholeiitic and alkalic basalt throughout its eruptive history (Fig. 1). In major and trace element plots, the tholeiites form trends that indicate fractionation, but the alkalic basalts form a separate group and do not follow these trends.

Tholeiitic and alkalic basalt are often seen together at other shield volcanoes where alkalic basalt overlies tholeiite. At Los Mogotes, however, tholeiite and alkalic basalt are interlayered, having been erupted from the same vents. This not only suggests the presence of two separate magma chambers beneath the mountain, but also a complex system of feeder dikes that would allow rising magma from both chambers to be erupted from the same vent at different times.

A fractional crystallization model was developed to evaluate variation among Los Mogotes tholeiites, but it was inconsistent with the modal abundances of phenocrysts in the basalts. In addition, a trace element test of the model, assuming that Rb, Zr, Sr, and Ba were completely incompatible, produced a range of incompatible trace elements that was much greater than could be accounted for by the fractional crystallization modeling (Fig. 2). This indicates that tholeiitic basalt from Los Mogotes is anomalously enriched in incompatible trace elements. These inconsistencies suggest that processes other than fractionation affected the composition of the lavas that were erupted.

Two processes could have combined with fractionation to cause the amount of variation among major and trace elements in these basalts. Any explanation requires the mixing of tholeiitic magma with a more evolved magma or rock to account for the enriched trace element values. Los Mogotes is located adjacent to two major volcanic fields (the San Juan and the Taos Plateau Volcanic Fields), both of which were active around the same time as Los Mogotes. This location provided opportunity for feeder dikes from its basaltic magma chambers to mingle with those from more evolved magma chambers. A second means to account for incompatible trace element enrichment of tholeiitic basalt at Los Mogotes is assimilation of upper crustal rocks, through which basalt had to pass and in which a tholeiitic magma chamber may have been located.

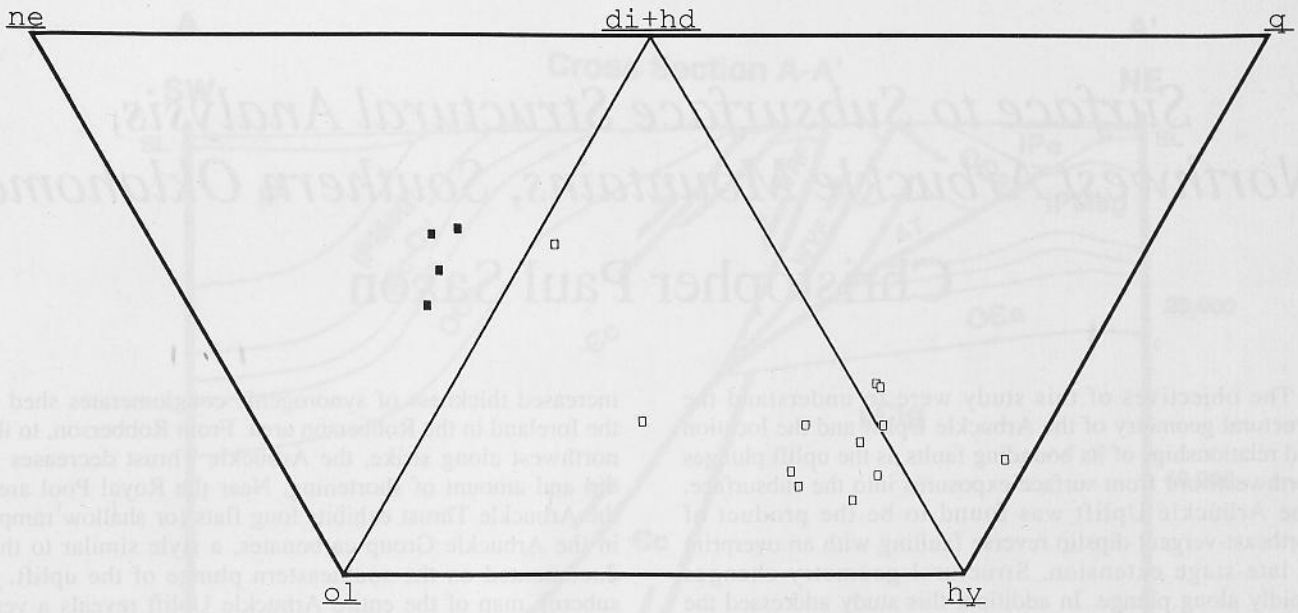

Fig. 1. The Los Mogotes Volcano produced both alkalic and tholeiitic lavas throughout its eruptive history. Analyzed samples are plotted in the basalt quadrilateral. Samples in the ne-di+hd-ol triangle are alkalic basalts, and are represented by filled squares. Tholeiites are shown with open squares. The samples fall into two distinct groups, indicating that there was little mixing between alkalic and tholeiitic magmas, though they were erupted from the same vents.

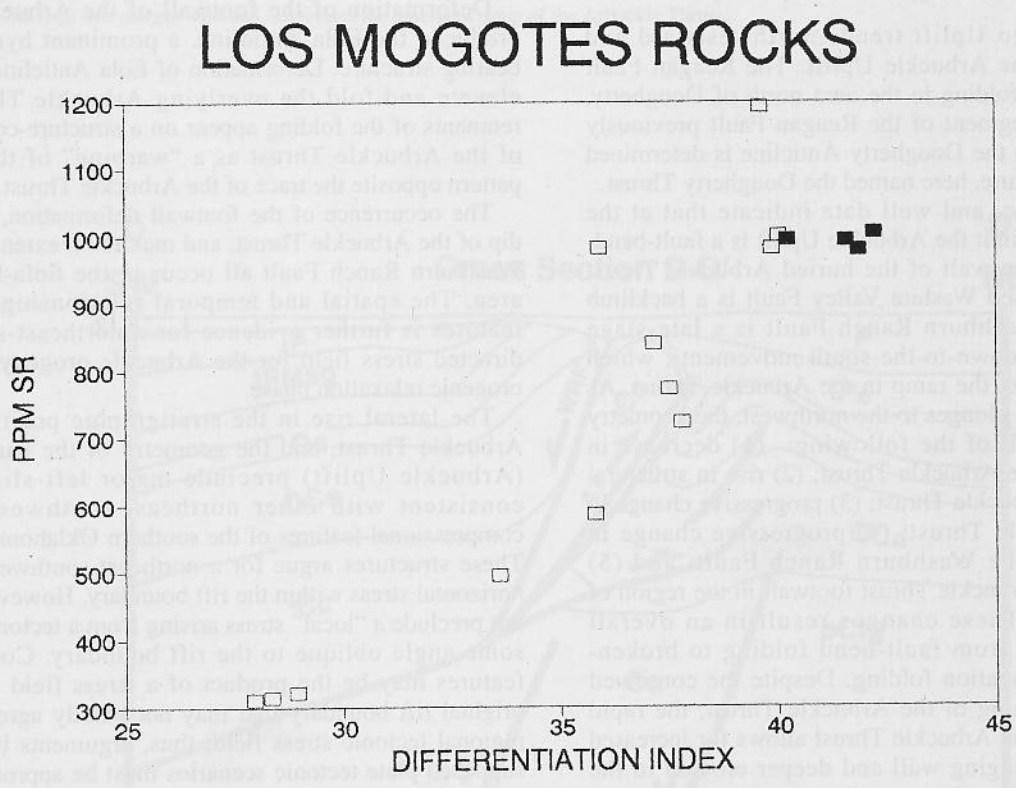

Fig. 2. A plot of Sr vs. D.I., the differentiation index for Los Mogotes rocks. D.I. is the sum of the normative constituents q + ab + or + ne + kp + lc. Alkalic samples are represented by filled squares and tholeiites are shown by open squares. The tholeiites show a variation of 400% in Sr concentration. This is much more than the fractionation model that was developed to evaluate variation among the tholeiites only allowed for, assuming that Sr behaves incompatibly. Sr readily substitutes for Ca in plagioclase feldspar. The model required more than 16% plagioclase fractionation to attain the amount of variation present in Los Mogotes samples. If the model were correct, and fractionation was the only process affecting magma composition, Sr should have been depleted with respect to the differentiation index.

Surface to Subsurface Structural Analysis, Northwest Arbuckle Mountains, Southern Oklahoma

Christopher Paul Saxon

The objectives of this study were to understand the structural geometry of the Arbuckle Uplift and the location and relationships of its bounding faults as the uplift plunges northwestward from surface exposures into the subsurface. The Arbuckle Uplift was found to be the product of northeast-vergent dipslip reverse faulting with an overprint of late-stage extension. Structural geometry changes rapidly along plunge. In addition, this study addressed the relationship of the Tishomingo Uplift to the Arbuckle Uplift.

The Arbuckle Uplift is the dominant surface expression of a series of basement-cored, northeast-vergent, northwest-trending uplifts of Pennsylvanian age comprised by the southern Oklahoma foreland. The area of investigation focuses on the western-most surface exposure of the Arbuckle Uplift, which continues at a northwest plunge in the subsurface to just west of the Royal Pool area (Tps. 1 N-2 S, and Rs. 1-4 W, Carter, Murray, and Stephens Counties).

The Tishomingo Uplift trends northwestward and plunges beneath the Arbuckle Uplift. The Reagan Fault dies out into tight folding in the area north of Dougherty, Oklahoma. The segment of the Reagan Fault previously mapped adjacent to the Dougherty Anticline is determined to be a separate feature, here named the Dougherty Thrust.

Surface, seismic, and well data indicate that at the northwest outcrop limit the Arbuckle Uplift is a fault-bend-fold on the hanging wall of the buried Arbuckle Thrust (Fig. 1). The exposed Washita Valley Fault is a backlimb imbricate. The Washburn Ranch Fault is a late-stage extensional fault (down-to-the-south movement), which merges at depth with the ramp in the Arbuckle Thrust. As the Arbuckle Uplift plunges to the northwest, the geometry changes as a result of the following: (1) decrease in shortening along the Arbuckle Thrust; (2) rise in structural elevation of the Arbuckle Thrust; (3) progressive change in dip of the Arbuckle Thrust; (4) progressive change in displacement in the Washburn Ranch Fault; and (5) shortening of the Arbuckle Thrust footwall in the region of Eola Oil Field. These changes result in an overall geometric change from fault-bend folding to broken-through fault-propagation folding. Despite the continued decrease in shortening of the Arbuckle Thrust, the rapid increase in dip of the Arbuckle Thrust allows for increased elevation of the hanging wall and deeper erosion to the level of the Cambrian "basement" in the Robberson area (Fig. 2). The increase in elevation contributes to the increased thickness of synorogenic conglomerates shed to the foreland in the Robberson area. From Robberson, to the northwest along strike, the Arbuckle Thrust decreases in dip and amount of shortening. Near the Royal Pool area, the Arbuckle Thrust exhibits long flats (or shallow ramps) in the Arbuckle Group carbonates, a style similar to that documented on the southeastern plunge of the uplift. A subcrop map of the entire Arbuckle Uplift reveals a very symmetrical compressive structure.

The Washburn Ranch Fault forms an arcuate subcrop trace, concave to the southwest, with maximum extension at the apex at the southern boundary of the Robberson area. The Washburn Ranch Fault post-dates the latest Virgillian compression, but pre-dates the overlying Permian sediments. The arcuate trace and location of the Washburn Ranch Fault above and behind the basement ramp of the Arbuckle Thrust indicate that it is probably listric at depth, having reactivated along the ramp of the Arbuckle Thrust.

Deformation of the footwall of the Arbuckle Thrust produced the Eola Anticline, a prominent hydrocarbon-bearing structure. Deformation of Eola Anticline helped to elevate and fold the overlying Arbuckle Thrust. The remnants of the folding appear on a structure-contour map of the Arbuckle Thrust as a "warping" of the contour pattern opposite the trace of the Arbuckle Thrust.

The occurrence of the footwall deformation, maximum dip of the Arbuckle Thrust, and maximum extension on the Washburn Ranch Fault all occur in the Eola-Robberson area. The spatial and temporal relationships of these features is further evidence for a northeast-southwest-directed stress field for the Arbuckle orogeny and post-orogenic relaxatlon phase.

The lateral rise in the stratigraphic position of the Arbuckle Thrust, and the geometry of the hanging wall (Arbuckle Uplift) preclude major left-slip and are consistent with other northeast-southwest-verging compressional features of the southern Oklahoma foreland. These structures argue for a northeast-southwest-directed horizontal stress within the rift boundary. However, they do not preclude a "local" stress arising from a tectonic stress at some angle oblique to the rift boundary. Compressive features may be the product of a stress field within the original rift boundary that may not wholly agree with the regional tectonic stress field; thus, arguments based upon supposed plate tectonic scenarios must be approached with extreme caution and a certain amount of skepticism.

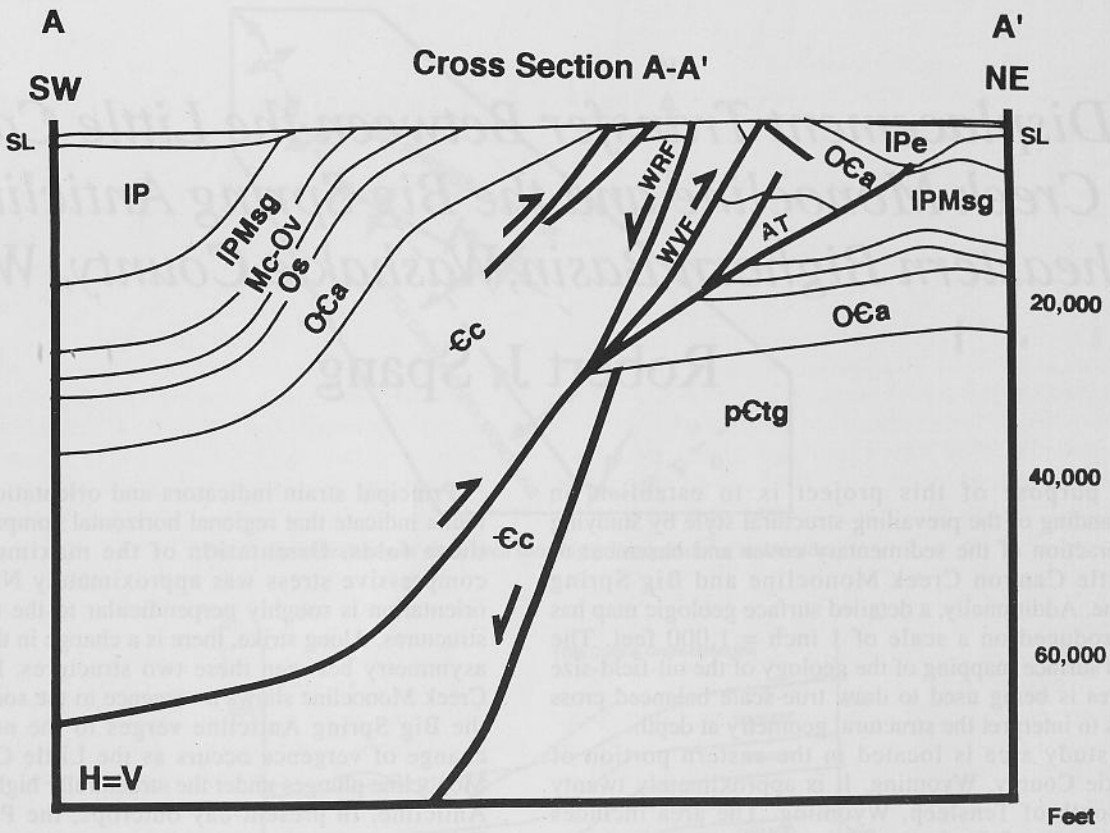

Fig. 1. Cross section A-A¢ is along the exposed Arbuckle Anticline. At this location, the Arbuckle Uplift is a fault-bend fold on the hanging wall of the Arbuckle Thrust. The Washita Valley Fault is a back-limb imbricate to the Arbuckle Thrust. Displacement is minor along the Washburn Ranch Fault, a late-stage extensional fault that merges with and reactivates the basement ramp of the Arbuckle Thrust.

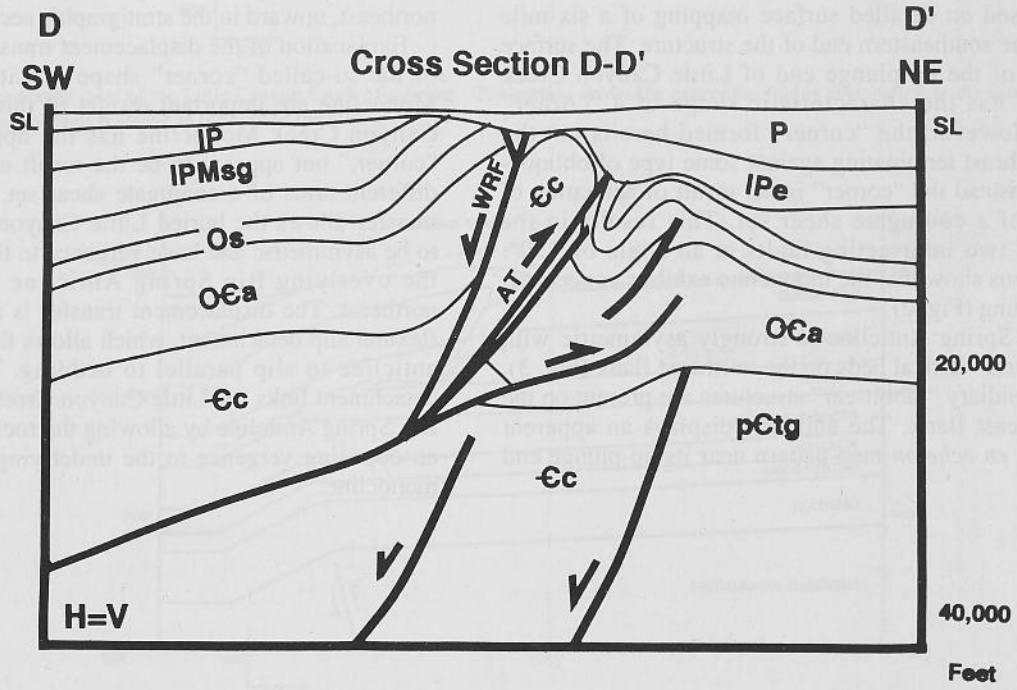

Fig. 2. Cross section D-D¢ (approximately 11 miles northwest of A-A¢) along the Eola portion of the Arbuckle Uplift. The Arbuckle Uplift geometry is that of a broken-through fault-propagation fold, overprinted with late-stage extension. In this area the footwall is shortened, forming Eola Anticline, a prolific hydrocarbon-bearing structure.

A Displacement Transfer Between the Little Canyon Creek Monocline and the Big Spring Anticline, Southeastern Bighorn Basin, Washakie County, Wyoming

Robert J. Spang

The purpose of this project is to establish an understanding of the prevailing structural style by studying the interaction of the sedimentary cover and basement of the Little Canyon Creek Monocline and Big Spring Anticline. Additionally, a detailed surface geologic map has been produced on a scale of 1 inch = 1,000 feet. The detailed surface mapping of the geology of the oil-field-size structures is being used to draw true-scale balanced cross sections to interpret the structural geometry at depth.

The study area is located in the eastern portion of Washakie County, Wyoming. It is approximately twenty miles south of Tensleep, Wyoming. The area includes portions of four 7.5-minute topographic quadrangle sheets. The area is also located adjacent to the Big Trails Fault system, which separates the Bighorn Basin from the Casper Arch to the southeast.

The Little Canyon Creek Monocline and the Big Spring Anticline, located in the southeastern Bighorn Basin, Wyoming, were formed during the Laramide orogeny. The Little Canyon Creek Monocline dips to the southwest and plunges to the northwest (Fig. 1). The monocline is mappable for at least 15 miles to the northwest, but this study is based on detailed surface mapping of a six-mile section at the southeastern end of the structure. The surface expression of the up-plunge end of Little Canyon Creek Monocline has the characteristic shape of a "corner" problem. However, the "corner" formed here is not the result of a thrust terminating against some type of oblique-slip fault. Instead the "corner" is the result of activation of two arms of a conjugate shear set. This results in the creation of two intersecting faults at an angle of 150°. Cross sections show that the monocline exhibits concentric, parallel folding (Fig. 2).

The Big Spring Anticline is strongly asymmetric with vertical to near-vertical beds on the northeast flank (Fig. 3). Several subsidiary "rabbit-ear" structures are present on the steep northeast flank. The anticline displays an apparent leftstepping *en echelon* map pattern near its up-plunge end (Fig. 1).

Principal strain indicators and orientation of primary faults indicate that regional horizontal compression caused these folds. Orientation of the maximum principle compressive stress was approximately N. 38° E. This orientation is roughly perpendicular to the trend of these structures. Along strike, there is a change in the direction of asymmetry between these two structures. Little Canyon Creek Monocline shows a vergence to the southwest, while the Big Spring Anticline verges to the northeast. The change of vergence occurs as the Little Canyon Creek Monocline plunges under the structurally higher Big Spring Anticline. In present-day outcrops, the Pennsylvanian Tensleep forms the west-facing crest of the Little Canyon Creek Monocline. An east-vergent thrust, which lifts the Pennsylvanian Tensleep Sandstone up the gentle back limb of Big Spring Anticline, suggests that the change of vergence occurs beneath the Pennsylvanian Tensleep Sandstone (Fig. 3). The change in asymmetry indicates that this area represents a displacement transfer zone. When projected into a single section down-plunge, the displacement transfer can be seen in a vertical sense as the direction of vergence changes from southwest at depth, to northeast, upward in the stratigraphic section.

Explanation of the displacement transfer and description of the so-called "corner" shape of Little Canyon Creek Monocline are important results of this study. The Little Canyon Creek Monocline has the apparent shape of a "corner," but appears to be the result of the activation of different arms of a conjugate shear set. The displacement transfer allows the buried Little Canyon Creek Monocline to be asymmetric and have vergence to the southeast, while the overlying Big Spring Anticline is vergent to the northeast. The displacement transfer is accomplished by a flexural slip detachment, which allows the rock units of the anticline to slip parallel to bedding. This flexural slip detachment links the Little Canyon Creek Monocline to the Big Spring Anticline by allowing the rocks to slip and show an opposing vergence to the underlying rock units of the monocline.

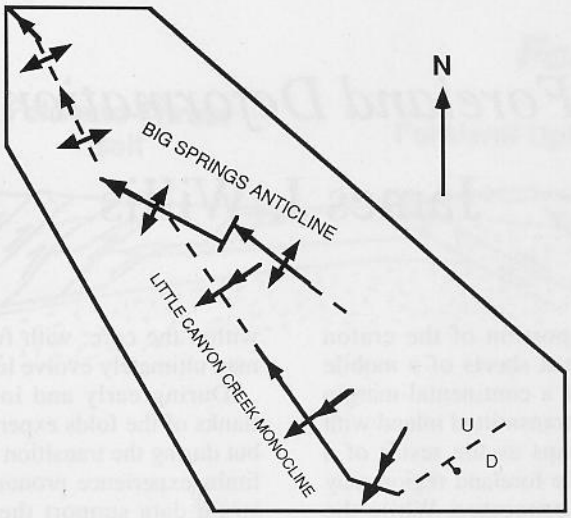

Fig. 1. Structural map of study area showing primary features and trends.

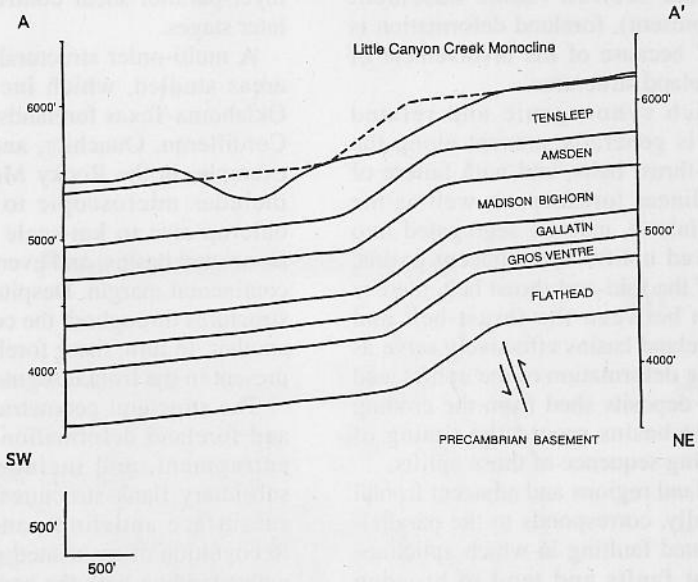

Fig. 2. Cross section across the crest of the Little Canyon Creek Monocline. The section shows the concentric fold is asymmetric to the southwest. Some form of high-angle basement fault is shown in the core of the fold.

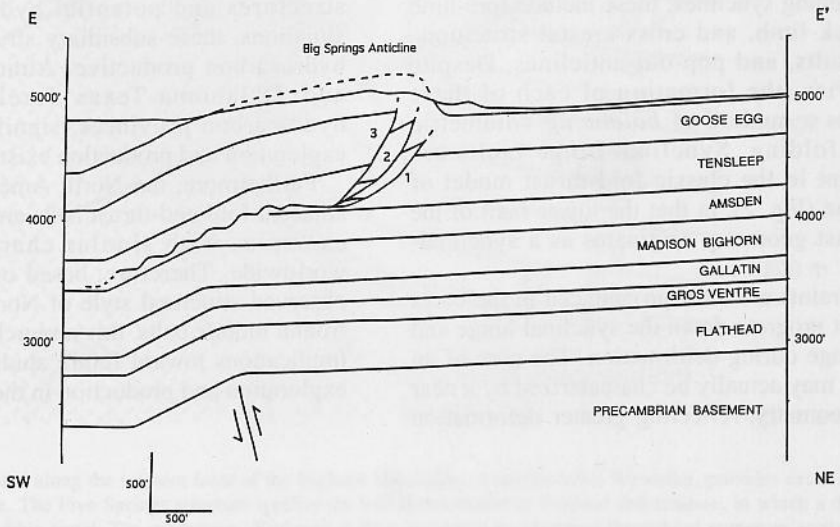

Fig. 3. Cross section across the crest of the Big Spring Anticline. The northeast asymmetry of the anticline seen at the surface changes with the presence of a detachment at depth. Below this detachment the asymmetry seen in Figure 2 is present.

Foreland Deformation

James J. Willis

The "foreland" represents the portion of the craton toward and onto which the overthrust sheets of a mobile belt advance during deformation of a continental-margin geosyncline (Fig. 1). As stresses are transmitted inland with progressive crustal collision, perhaps as the result of a flattening in the subduction angle, the foreland region may become involved in the orogenic processes. While the frontal portions of fold-and-thrust belts are considered to be "thin-skinned" due to the involvement, primarily, of the geosynclinal stratigraphic section (some basement involvement may also be present), foreland deformation is considered "thick-skinned" because of the involvement of basement rocks in most foreland structures.

A foredeep, into which synorogenic and related sediments are deposited, is generally present along the frontal margin of fold-and-thrust belts, and with failure of the craton this extensive linear foredeep, as well as the cratonic sequence further inland, may be segregated into numerous basement-involved uplifts and adjacent basins. Along the frontal margin of the fold-and-thrust belt, there is commonly an interaction between the thrust-belt and foreland structures. The foreland basins effectively serve as localized depocenters during deformation of the uplifts, and the associated synorogenic deposits shed from the eroding uplifted highlands into the basins record the timing of deformation and the unroofing sequence of those uplifts.

Deformation within foreland regions and adjacent frontal fold-and-thrust belts generally, corresponds to the parallel-style of folding and associated faulting in which anticlines are cored by major thrust faults and tend to broaden upsection, whereas synclinal elements tighten upsection. Several smaller-scale subsidiary structures are associated with parallel folding and the related volumetric constriction in the upward-tightening synclines; these include fore-limb ("rabbit-ear"), back-limb, and cross-crestal structures, synclinal-hinge faults, and pop-out anticlines. Despite different geometries, the formation of each of these structures provides a method of *balancing* volumetric problems during folding. Synclinal-hinge faults are especially important in the classic fold-thrust model of foreland deformation (Fig. 2), in that the lower fault of the dual-fault fold-thrust geometry originates as a synclinal-hinge fault.

Volumetric constraints are most pronounced in the cores of parallel folds, but progress down the synclinal hinge and up the anticlinal hinge during deformation. The core of an overall parallel fold may actually be characterized by a near similar-style fold geometry, reflecting greater deformation within the core; with further deformation, the entire fold may ultimately evolve into a similar-type fold.

During early and intermediate stages of folding, the flanks of the folds experience localized tectonic thickening, but during the transition from parallel to similar folding, the limbs experience pronounced tectonic thinning. Stress and strain data support the observed style and sequence of deformation—layer-parallel shortening is clearly important during early and intermediate stages of folding, whereas layer-parallel shear contributes predominantly during the later stages.

A multi-order structural continuum was observed in the areas studied, which include the Rocky Mountain and Oklahoma-Texas forelands, and the frontal segments of the Cordilleran, Ouachita, and Appalachian thrust belts. For example, in the Rocky Mountain foreland, the continuum includes microscopic to small megascopic structures, outcrop-size to km-scale features, mountain uplifts and associated basins, and even the entire foreland and adjacent continental margin. Despite pronounced differences in size, structures throughout the continuum are quite similar to one another. In turn, these foreland structures reflect geometries present in the frontal segments of fold-and-thrust belts.

The structural geometries involved in frontal thrust-belt and foreland deformation are conducive to hydrocarbon entrapment, and include primary anticlinal closures, subsidiary flank structures, flank stratigraphic traps, blind subsurface anticlines, and a variety of subthrust traps. Recognition of associated subsidiary structures is critical to understanding both the geometry and deformational history of the primary structure. In many cases, the surface and shallow subsurface geometries are controlled by these secondary structures, in effect obscuring deeper subsurface structures and potential hydrocarbon traps. In other situations, these subsidiary structures may themselves be hydrocarbon productive. Although the Rocky Mountain and Oklahoma-Texas forelands represent mature hydrocarbon provinces, significant frontiers for future exploration and production exist in those regions.

Furthermore, the North American deformed craton and adjacent fold-and-thrust belts are not unique, and numerous examples with similar characteristics can be cited worldwide. Therefore, based on the pervasiveness of the observed structural style of North American forelands and frontal mobile belts, this research will likely have important implications toward future studies as well as hydrocarbon exploration and production in the international arena.

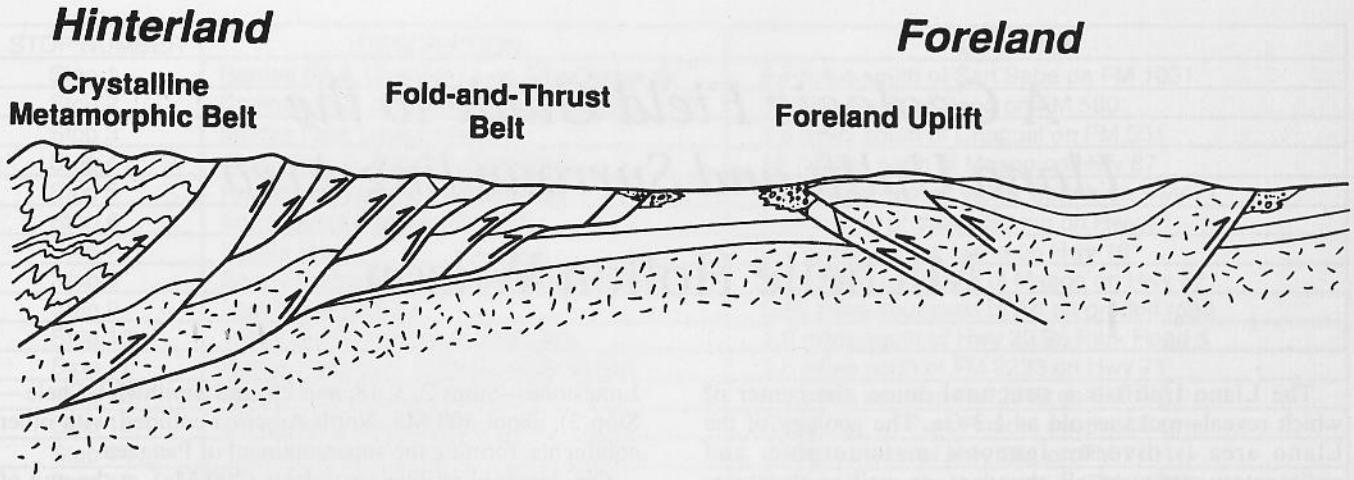

Fig. 1. Schematic cross section of a deformed mobile belt and adjacent foreland, showing the typical transition from a crystalline metamorphic belt to a "thin-skinned" fold-and-thrust belt to the deformed foreland or craton. Individual uplifts may serve as source areas for synorogenic sediments deposited into adjacent basinal depocenters.

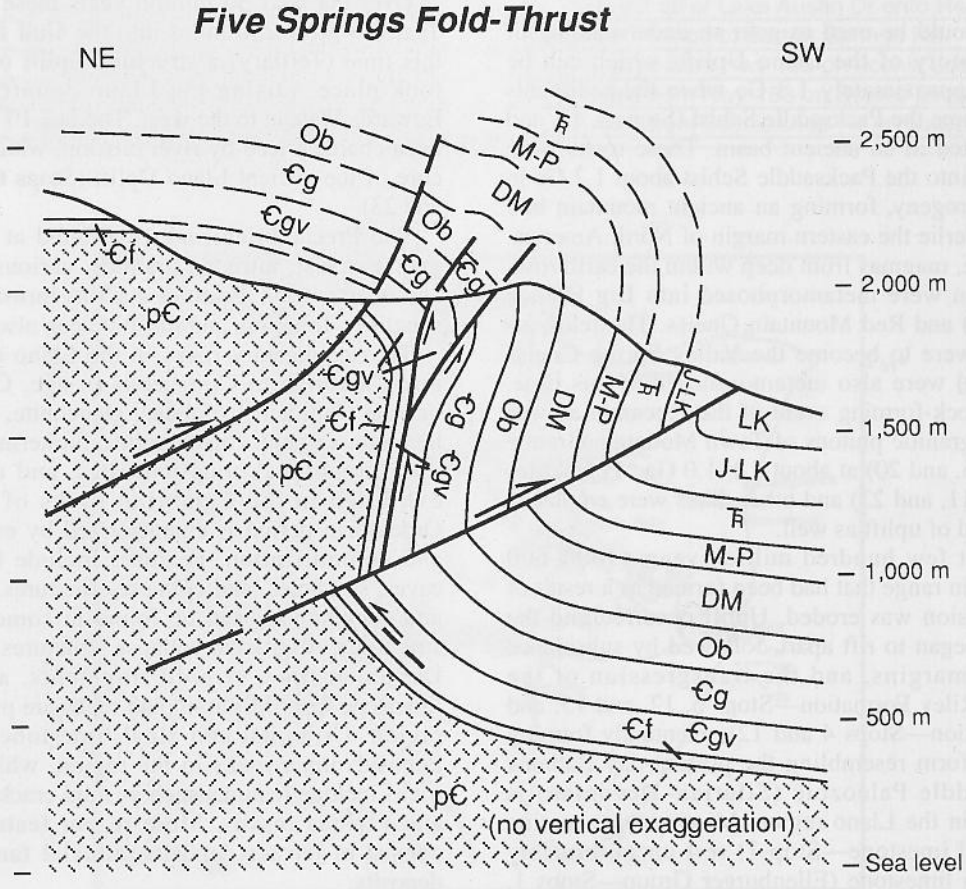

Fig. 2. The Five Springs area, located along the western front of the Bighorn Mountains of north-central Wyoming, provides excellent exposure of a classic Rocky Mountain foreland structure. The Five Springs structure typifies the fold-thrust model of foreland deformation, in which a dual-fault system bounds an overturned and thinned stratigraphic panel. The geometries displayed at Five Springs were observed throughout numerous tectonic provinces, including elsewhere in the Rocky Mountain foreland, in the Oklahoma-Texas foreland, and in the frontal segments of various mobile belts. These and related geometries were also observed over a wide range in size, from microscopic examples to the continental margins.

A Geologic Field Guide to the Llano Uplift and Surrounding Area

Michelle Hollon Wilson

The Llano Uplift is a structural dome, the center of which reveals rocks as old as 1.3 Ga. The geology of the Llano area is diverse: igneous, metamorphic, and sedimentary rocks are all abundant, as well as structures such as faults and folds. The Llano Uplift is located in Central Texas, northwest of Austin. It is bounded on the east and south by the Balcones Fault Zone and the buried Ouachita Mountain belt and on the north and west by the Bend Arch.

This study consists of a field guide, written expressly for secondary teachers, to thirty-two easily accessible stops in and around the Llano Uplift (Fig. 1) that illustrate, collectively, its geologic history. Also included are maps of how to reach the stops, features and collectibles that can be seen and gathered, and a summary of the geology at each stop.

This guide should be used to gain an understanding of the geologic history of the Llano Uplift, which can be traced back to approximately 1.3 Ga when the sediments that were to become the Packsaddle Schist (Stops 8, 11, and 20) were deposited in an ancient basin. These rocks were metamorphosed into the Packsaddle Schist about 1.2 Ga in the Greenville orogeny, forming an ancient mountain belt whose rocks underlie the eastern margin of North America. At the same time, magmas from deep within the earth rose, crystallized, then were metamorphosed into Big Branch Gneiss (Stop 23) and Red Mountain Gneiss. The feldspar-rich rocks that were to become the Valley Spring Gneiss (Stops 6 and 10) were also metamorphosed at this time. The last major rock-forming event of the Precambrian was the intrusion of granitic plutons of Town Mountain Granite (Stops 14, 15, 16, and 20) at about 1.1–1.0 Ga. Pegmatites (Stops 7, 8, 10, 11, and 23) and other dikes were emplaced during this period of uplift as well.

Over the next few hundred million years (1000–600 Ma), the mountain range that had been formed as a result of continental collision was eroded. Uplift occurred and the two continents began to rift apart, followed by subsidence of the faulted margins, and the transgression of the Cambrian Sea (Riley Formation—Stops 5, 12, and 15; and Wilberns Formation—Stops 4 and 12), eventually forming a carbonate platform resembling the present-day Bahama Banks. The middle Paleozoic (Silurian–Devonian) is virtually absent in the Llano region. Mississippian marine rocks (Chappel Limestone—Stop 1) rest unconformably upon Ordovician limestone (Ellenburger Group—Stops 1, 17, and 19). During the Pennsylvanian (Marble Falls Limestone—Stops 2, 3, 18, and 25, and Smithwick Shale—Stop 2), about 300 Ma, North America collided with other continents, forming the supercontinent of Pangaea.

One hundred million years later (200 Ma), at the end of the Triassic (Sycamore Conglomerate—Stops 19 and 25), Pangaea split apart. The southern part of the North American continent sagged and the early Gulf of Mexico began to form south and southeast of the Llano area during the Jurassic period. Once again, subsidence occurred and transgressing Cretaceous Seas deposited marine sediments (Hammet Shale and Cow Creek Limestone—Stop 26; and Glen Rose Limestone—Stop 32) over Central Texas. Then, at 60 Ma, the gulf began to sag more rapidly as sandy and muddy sediments began to pour in from the rising Rocky Mountains to the northeast.

Over the next 50 million years these sediments caused Texas to grow 250 miles into the Gulf of Mexico. During this time (Tertiary) a structural uplift of about 2000 feet took place, raising the Llano country, as well as the Edwards Plateau to the west. The last 10 million years have been characterized by river erosion, which has exposed the core of the ancient Llano Uplift (Stops 6, 8, 9, 10, 11, 20, and 23).

The Precambrian rocks exhibited at the stops include gneiss, schist, intruded granites, various pegmatite dikes, and quartz veins. Features such as thrust faults, anticlines, synclines, foliation, and lineation can also be seen.

The sedimentary rocks in the Llano region range from mid-Cambrian to Cretaceous in age. Cambrian features include ventifacts, trilobites, glauconite, crossbedding, and hematite cement. Stromatolitic bioherms and biostromes, intraformational conglomerates, and dolomite are also exhibited in the Cambrian rocks of the region. The Ordovician period is characterized by extensive limestone and dolomitization. Features include karst topography, caves, sinkholes, and collapse structures. Well-worn corals and cephalopods can be found in some of the collapsed structures. Additional collapse structures from Silurian and Devonian time, crinoid fragments, and petroliferous limestone from Mississippian rocks are present in the Llano region. Crinoidal and algal limestone can be found in Pennsylvanian rocks in the region, while the Cretaceous rocks include features such as mud cracks, dinosaur tracks, and various fossils. More recent features of the Llano consist of terrace deposits, alluvial fans, and floodplain deposits.

STOP NUMBER	DESCRIPTION	LOCATION
Stop 1	Barnett Sh & Chappel Ls on Ellenburger Gr	2.7 miles south of San Saba on FM 1031
Stop 2	Smithwick Sh overlying Marble Falls Ls	.9 miles south of Bend on FM 580
Stop 3	Marble Falls Limestone	1.8 miles south of Chappel on FM 501
Stop 4	Algal reefs in Wilberns Formation	18.7 miles north of Mason on Hwy 87
Stop 5	Hickory Sandstone with hematite	14.7 miles west of Valley Spring on Hwy 71
Stop 6	Iron Mountain Magnetite Mine	1 mile west of Valley Spring on Hwy 71
Stop 7	Llanite Dike	9.7 miles north of Llano on Hwy 16
Stop 8	Sandy Formation of Packsaddle Schist	2.75 miles southeast of Mason on Hwy 87
Stop 9	Lost Creek Gneiss	6.55 miles southeast of Art on graded road
Stop 10	Valley Spring Gneiss at Inks Lake	1.8 miles south of Hwy 29 9n Park Road 4
Stop 11	Honey Formation of Packsaddle Schist	3.5 miles north of FM 2233 on Hwy 71
Stop 12	Riley and Wilberns Formations	1.1 miles south of FM 2342 on FM 1431
Stop 13	Longhorn Caverns State Park	Off of 281 on Park Road 4 south of Burnet
Stop 14	Town Mountain Granite	1.8 miles west of Hwy 281 on FM 1431
Stop 15	Hickory Ss on Town Mountain Granite	3 miles from granite quarry on FM 1431
Stop 16	Fault of Marble Falls Ls & Town Mtn Gran.	1.2 miles west of Hwy 281 on FM 1431
Stop 17	Ellenburger Group	1 mile south of Marble Falls, take road to dam
Stop 18	Max Starke Dam overlook	1 mile south of Marble Falls, take road to dam
Stop 19	Collapsed singhole in Ellenburger Group	4.3 miles south of FM 1431 on Hwy 281
Stop 20	Enchanted Rock State Park	17 miles north of Fredricksburg on RR 965
Stop 21	Oatman Creek Granite	3.9 miles north of Hwy 290 on RR 965
Stop 22	Willow City Loop	2.7 miles west of Hwy 16 on FM 1323
Stop 23	Big Branch Gneiss	2.5 miles N of FM 1323 on Althus-Davis Rd.
Stop 24	Glen Rose fossils near Blano	CR 112, off FM 1623, 1.1 miles from Blanco
Stop 25	Pedernales Falls State Park	9.4 miles from Johnson City on FM 2766
Stop 26	Cow Creek Ls and Hammett Sh	8 miles southwest of Hwy 71 on FM 2766
Stop 27	Edwards Ls outcrop on Colorado River	Turn left off of Lake Austin Dr onto Red Bud Tr.
Stop 28	Barton Springs	Zilker Park off of Barton Springs Rd.
Stop 29	Pilot's knob volcano	1.5 miles from Hwy 183 on scenic Loop Rd
Stop 30	McKinney Falls State Park	2 miles from Hwy 183 on Scenic Loop Rd
Stop 31	Nepheline Basanite (basalt)	.7 miles from Scenic Loop Rd on cotton-Buff Springs Rd

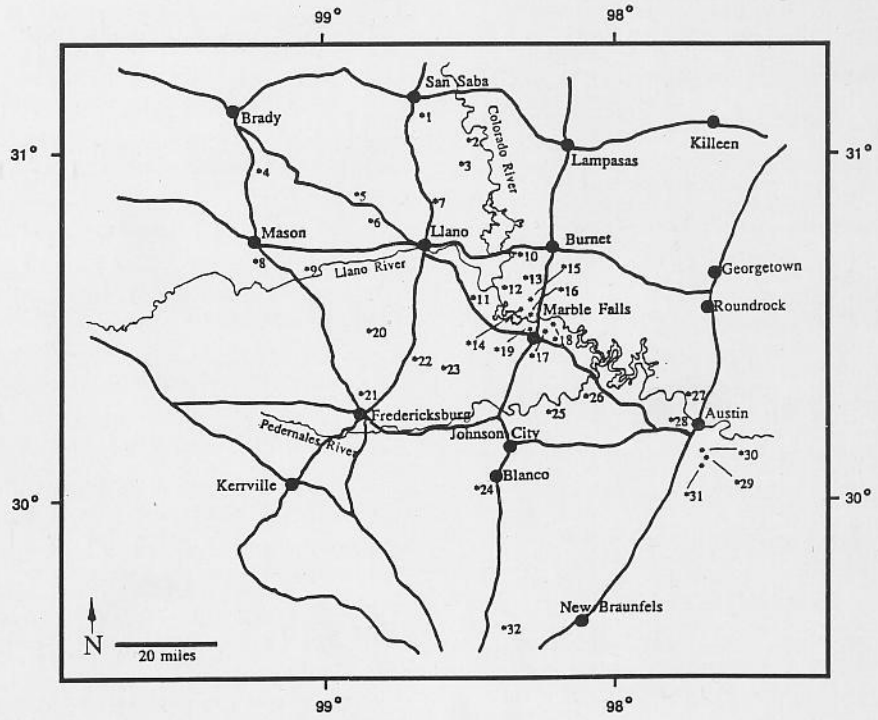

Fig. 1. Descriptions and locations of stops in the field guide (stop 32, Natural Bridge Caverns, occurs south of the map and could not be shown due to space limitations, but it is easy to find on FM 3009 west of New Braunfels).

STOP NUMBER	DESCRIPTION	LOCATION
Stop 1		
Stop 2		
Stop 3		
Stop 4		
Stop 5		
Stop 6		
Stop 7		
Stop 8		
Stop 9		
Stop 10		
Stop 11		

BAYLOR GEOLOGICAL PUBLICATIONS

Baylor Geological Studies

1. Holloway, Harold D., 1961, The Lower Cretaceous Trinity aquifers, McLennan County, Texas: Baylor Geological Studies Bulletin No. 1 (Fall). *Out of print.*
2. Atlee, William A., 1962, The Lower Cretaceous Paluxy Sand in central Texas: Baylor Geological Studies Bulletin No. 2 (Spring). *Out of print.*
3. Henningsen, E. Robert, 1962, Water diagenesis in Lower Cretaceous Trinity aquifers of central Texas: Baylor Geological Studies Bulletin No. 3 (Fall). *Out of print.*
4. Silver, Burr A., 1963, The Bluebonnet Member, Lake Waco Formation (Upper Cretaceous), central Texas, A lagoonal deposit: Baylor Geological Studies Bulletin No. 4 (Spring). *Out of print.*
5. Brown, Johnnie B., 1963, The role of geology in a unified conservation program, Flat Top Ranch, Bosque County, Texas: Baylor Geological Studies Bulletin No. 5 (Fall). *Out of print.*
6. Beall, Arthur O., Jr., 1964, Stratigraphy of the Taylor Formation (Upper Cretaceous), east-central Texas: Baylor Geological Studies Bulletin No. 6 (Spring). *Out of print.*
7. Spencer, Jean M., 1964, Geologic factors controlling mutations and evolution—A review: Baylor Geological Studies Bulletin No.7 (Fall). *Out of print.*

** 8. Part I: Geology, 1965, Geology and urban development by Peter T. Flawn; Geology of Waco by J. M. Burket: Baylor Geological Studies Bulletin No. 8 (Spring). *Out of print.*

** 9 Part II: Soils, 1965, Soils and urban development of Waco by W. R. Elder: Baylor Geological Studies Bulletin No. 9 (Fall). $5.00.

**10. Part III: Water, 1966, Surface waters of Waco by Jean M. Spencer: Baylor Geological Studies Bulletin No. 10 (Spring). $5.00.

**11. Part III: Water, 1976, Subsurface waters of Waco by Siegfried Rupp: Baylor Geological Studies Bulletin No. 11 (Fall). $5.00.

**12. Part IV: Engineering, 1967, Geologic factors affecting construction in Waco by R. G. Font and E. F. Williamson: Baylor Geological Studies Bull. No. 12 (Spring). *Out of print.*

**13&14. Parts V & VI: 1992, Environmental Atlas of McLennan County by Joe C.Yelderman, Jr. and Robert E. Cervenka: Baylor Geological Studies Bulletin No. 13 & 14 (Spring). $25.00.

15. Boone, Peter A., 1968, Stratigraphy of the basal Trinity (Lower Cretaceous) sands, central Texas; Baylor Geological Studies Bulletin No. 15 (Fall) . $5 .00.
16. Proctor, Cleo V., 1969, The North Bosque watershed, Inventory of a drainage basin: Baylor Geological Studies Bulletin No. 16 (Spring). *Out of print.*
17. LeWand, Raymond L., Jr., 1969, The geomorphic evolution of the Leon River system: Baylor Geological Studies Bulletin No. 17 (Fall). *Out of print.*
18. Moore, Thomas H., 1970, Water geochemistry, Hog Creek basin, central Texas: Baylor Geological Studies Bulletin No. 18 (Spring). *Out of print.*
19. Mosteller, Moice A., 1970, Subsurface stratigraphy of the Comanchean Series in east central Texas: Baylor Geological Studies Bulletin No. 19 (Fall). *Out of print.*
20. Byrd, Clifford Leon, 1971, Origin and history of the Uvalde Gravel of central Texas: Baylor Geological Studies Bulletin No. 20 (Spring). *Out of print.*
21. Brown, Thomas E., 1971, Stratigraphy of the Washita Group in central Texas: Baylor Geological Studies Bulletin No. 21 (Fall). *Out of print.*
22. Thomas, Ronny G., 1972, The geomorphic evolution of the Pecos River system: Baylor Geological Studies Bulletin No. 22 (Spring). *Out of print.*
23. Roberson, Dana Shumard, 1972, The paleoecology, distribution and significance of circular bioherms in the Edwards Limestone of central Texas: Baylor Geological Studies Bulletin No. 23 (Fall). *Out of print.*
24. Epps, Lawrence Ward, 1973, The geologic history of the Brazos River: Baylor Geological Studies Bulletin No. 24 (Spring). *Out of print.*
25. Bain, James S., 1973, The nature of the Cretaceous-pre-Cretaceous contact in north-central Texas: Baylor Geological Studies Bulletin No. 25 (Fall). *Out of print.*
26. Davis, Keith W., 1974, Stratigraphy and depositional environments of the Glen Rose Formation, north-central Texas: Baylor Geological Studies Bulletin No. 26 (Spring). *Out of print.*
27. Baldwin, Ellwood E., 1974, Urban geology of the Interstate Highway 35 growth corridor between Belton and Hillsboro, Texas: Baylor Geological Studies Bulletin No. 27 (Fall). $5.00.
28. Allen, Peter M., 1975, Urban geology of the Interstate Highway 35 growth corridor from Hillsboro to Dallas County, Texas: Baylor Geological Studies Bulletin No. 28 (Spring). $5.00.
29. Belcher, Robert C., 1975, The geomorphic evolution of the Rio Grande: Baylor Geological Studies Bulletin No. 29 (Fall). $5.00.
30. Flatt, Carl Dean, 1976, Origin and significance of the oyster banks in the Walnut Clay formation, central Texas: Baylor Geological Studies Bulletin No. 30 (Spring). *Out of print.*
31. Dolliver, Paul Noble, 1976, The significance of Robert Thomas Hill's contribution to the knowledge of central Texas geology: Baylor Geological Studies Bulletin No. 31 (Fall). $5.00.
32. Pool, James Roy, 1977, Morphology and recharge potential of certain playa lakes of the Edwards Plateau of Texas: Baylor Geological Studies Bulletin No. 32 (Spring). $5.00.
33. Bishop, Arthur L., 1977, Flood potential of the Bosque basin: Baylor Geological Studies Bulletin No. 33 (Fall). $5.00.
34. Hayward, Chris, 1978, Structural evolution of the Waco region: Baylor Geological Studies Bulletin No. 34 (Spring). $5.00.
35. Walker, Jimmy R., 1978, Geomorphic evolution of the Southern High Plains: Baylor Geological Studies Bulletin No. 35 (Fall). $5.00.
36. Owen, Mark Thomas, 1979, The Paluxy Sand in north-central Texas: Baylor Geological Studies Bulletin No. 36 (Spring). $5.00.
37. Bammel, Bobby H., 1979, Stratigraphy of the Simsboro Formation, east-central Texas: Baylor Geological Studies Bulletin No. 37 (Fall). $5.00.
38. Leach, Edward Dale, 1980, Probable maximum flood on the Brazos River in the City of Waco: Baylor Geological Studies Bulletin No. 38 (Spring). $5.00.
39. Ray, Bradley S., 1980, A study of the crinoid genus *Camarocrinus* in the Hunton Group of Pontotoc County, Oklahoma: Baylor Geological Studies Bulletin No. 39 (Fall). *Out of print.*
40. Corwin, Linda Whigham, 1982, Stratigraphy of the Fredericksburg Group north of the Colorado River, Texas: Baylor Geological Studies Bulletin No. 40 (Spring). $5.00.
41. Gawloski, Ted, 1983, Stratigraphy and environmental significance of the continental Triassic rocks of Texas: Baylor Geological Studies Bulletin No. 41 (Spring). $5.00.
42. Dolliver, Paul N., 1984, Cenozoic evolution of the Canadian River Basin: Baylor Geological Studies Bulletin No. 42 (Spring). $5.00.
43. McKnight, Cleavy L., 1986, Descriptive geomorphology of the Guadalupe Mountains, south-central New Mexico and West Texas: Baylor Geological Studies Bulletin No. 43 (Spring). $5.00.
44. Matthews, Truitt F., 1986, The petroleum potential of "serpentine plugs" and associated rocks, central and south Texas: Baylor Geological Studies Bulletin No. 44 (Fall). $5.00.
45. Surles, Milton A., Jr., 1987, Stratigraphy of the Eagle Ford Group (Upper Cretaceous) and its source-rock potential in the East Texas Basin: Baylor Geological Studies Bulletin No. 45 (Fall). $5.00.
46. Rapp, Keith Burleigh, 1988, Groundwater recharge in the Trinity Aquifer, central Texas: Baylor Geological Studies Bulletin No. 46 (Spring). $5.00.
47. Anderson, L. Marlow, 1989, Stratigraphy of the Fredericksburg Group, East Texas Basin: Baylor Geological Studies Bulletin No. 47 (Spring). $5.00.
48. Fall, 1989, Thesis Abstracts: Baylor Geological Studies Bulletin No. 48. $5.00.
49. Hawthorne, J. Michael, 1990, Dinosaur track-bearing strata of the Lampasas Cut Plain and Edwards Plateau, Texas: Baylor Geological Studies Bulletin No. 49 (Spring). $5.00.
50. Fall, 1990, Thesis Abstracts: Baylor Geological Studies Bulletin No. 50 (Fall). $5.00.
51. Pettigrew, Robert J., Jr., 1991, Geology and flow systems of the Hickory aquifer, San Saba County, Texas: Baylor Geological Studies Bulletin No. 51 (Spring). $5.00.
52. Fall, 1991, Thesis Abstracts: Baylor Geological Studies Bulletin No. 52 (Fall). $5.00.
53. Fall, 1992, Thesis Abstracts: Baylor Geological Studies Bulletin No. 53 (Fall). $5.00.
54. Fall, 1994, Thesis Abstracts: Baylor Geological Studies Bulletin No. 54 (Fall), $5.00.
55. Spring, 1995, Geomorhic Response to Regional Structure, Lampasas Cut Plain, Central Texas: Baylor Geological Studies Bulletin No. 55 (Spring). $5.00.
56. Fall, 1995, Thesis Abstracts: Baylor Geological Studies Bulletin No. 56 (Fall), $5.00.

Baylor Geological Society

101-138, 147-149, 151: *Out of print.* For titles see earlier Baylor Geological Studies Bulletins.,

139. Urban development along the White Rock Escarpment, Dallas, Texas, 1978. $3.00.
140. Paluxy Basin: Geology of a river basin in north central Texas, 1979. $3.00.
141. Geomorphic evolution of the Grand Prairie, central Texas, 1979. $3.00.
142. The nature of the Cretaceous/pre-Cretaceous contact, central Texas, 1979. $4.00, a professional level guidebook.
143. The geology of urban growth, 1979. $3.00.
144. A day in the Cretaceous, 1980. $3.00.
145. Landscape and landuse, 1980. $3.00.
146. Southeastern Llano country, 1983. $3.00.
150. Pre-Pennsylvanian geology of the Arbuckle Mountain region, southern Oklahoma, 1987. $10.00.

* Publications available from Baylor Geology Department, Baylor University, Waco, Texas 76798. Prices include postage, handling and sales tax, except for Bulletins 13 &14 which require special mailing (add $5.00 if ordered by mail). Baylor Geological Studies bulletins out of print **may** be available as photo copies.

** Part of **Urban Geology of Greater Waco,** a series on urban geology in cooperation with Cooper Foundation of Waco.


BAYLOR UNIVERSITY
GEOLOGY